Supplementary Cementitious Materials in Portland Limestone Cements

Journal:	*ACI Structural and Materials Journals*
Manuscript ID	M-2021-122.R1
Journal Name:	ACI Materials Journal
Date Submitted by the Author:	n/a
Complete List of Authors:	Bharadwaj, Keshav; Oregon State University, School of Civil and Construction Engineering; Isgor, O. Burkan; Oregon State University, School of Civil and Construction Engineering Weiss, Jason; Oregon State University, Civil Engineering
Keywords:	supplementary cementitious materials, clinker, limestone, portland limestone cement, thermodynamic modeling

Supplementary Cementitious Materials in Portland Limestone Cements

by Keshav Bharadwaj, O. Burkan Isgor, and W. Jason Weiss

Biography:

ACI member **Keshav Bharadwaj** is a Ph.D. Student at Oregon State University, Corvallis, Oregon. He received his M. Tech. in Applied Mechanics and B. Tech. in Civil Engineering from the Indian Institute of Technology Madras, Chennai, India. His research interests include thermodynamic modeling, reactivity, transport in cementitious systems, and linking the microstructure of concrete to the engineering performance of concrete.

O. Burkan Isgor, FACI, is a professor in the School of Civil and Construction Engineering at Oregon State University, Corvallis, Oregon. He is the chair of ACI Committee 222, Corrosion of Metals in Concrete, and a member of ACI Committees 236, Material Science of Concrete, and 365, Service Life Prediction. His research interests include corrosion of steel in concrete, service-life modeling, and nondestructive testing.

Jason Weiss, FACI, is the Edwards Distinguished Professor of Engineering in the School of Civil and Construction Engineering at Oregon State University, Corvallis, Oregon. He is Editor in Chief of the ACI Materials Journal and a Member of the ACI Board.

ABSTRACT

Thermodynamic modeling was used to study the performance of portland-limestone cements (PLC) when it was combined with supplementary cementing material (SCM). The type of cement (i.e., I, II, III, V) did not substantially affect the porosity; however, cements with a greater alumina content, resulted in more ettringite formation than low alumina cements in systems with similar porosity. Alumina in clinker or SCM was predicted to react with calcite to form hemi/monocarbonate phases when calcium hydroxide is available, and stratlingite if calcium hydroxide is depleted. The decrease in the porosity was greater in the PLC+metakaolin systems due to the higher available reactive alumina than PLC+fly ash and PLC+slag systems. SCMs can be beneficially used with PLC.

Keywords: Supplementary Cementitious Materials; Clinker; Limestone; Portland Limestone Cement; Thermodynamic modeling.

INTRODUCTION

The use of portland-limestone cements (PLC) as a replacement for ordinary portland cement (OPC) in concrete has been gaining momentum due to inherent environmental benefits associated with the reduction of CO_2 emissions during production (1, 2). ASTM C150/ASHTO M85 typically allows up to 5% ground limestone content in OPCs (3, 4), and ASTM C595/AASHTO M240 permits up to 15% limestone additions to the clinker (1, 5-7). Although some consider limestone an inert material, it can affect the reaction products of hydrated OPC systems (7-12). For example, in typical OPC systems, limestone content can stabilize ettringite and result in the formation of monocarbonate instead of monosulfate (8, 9, 12-14). This change in the phase assemblage of reaction products due to the presence of limestone can sometimes directly impact the porosity and pore volume distribution in concrete as ettringite is a more space-filling phase (1, 15). Matschei et al. (15) showed that the porosity of OPC-Limestone systems decreased (accompanied by an increase in compressive strength) when the limestone content increased from 0% to 2%, but any further increase in limestone content led to an increase in the porosity above the minimum porosity (and a decrease in compressive strength). It is worth noting that even at a 15% limestone content, the porosity of PLC systems is lower than the porosity of an OPC system with 0% limestone (15). Several authors have then experimentally studied the synergistic effect of using alumina containing supplementary cementitious materials (SCMs) such as fly ash or metakaolin with limestone on the compressive strength of concrete (14, 16).

This work studies the impact of clinker chemistry and SCM addition on the reaction products and porosity of OPC-limestone systems. Concrete performance can be related to its porosity, pore volume distribution, and the chemical composition of its hydrated phases and pore solution. Porosity is a key feature that can be related to engineering properties (17). For example,

the strength of concrete made with OPC has been historically related to the water-to-cement ratio (w/c) through models such as Abram's model (18), Bolomey's model (19), or Feret's model (20). In these models, w/c was mainly used as a surrogate for the porosity of concrete. In recent years, Thermodynamic modeling has gained popularity as a tool to predict reaction products and porosity in cementitious systems (8, 21-23). Thermodynamic modeling has also been coupled with the Powers-Brownyard model to accurately calculate the porosity of pastes made of OPC (24) and OPC-SCM mixtures (25). The Powers-Brownyard model accounts for pores of two sizes (gel and capillary) in OPC systems using the gel-to-space ratio to predict the compressive strength (26, 27). The Powers-Brownyard approach coupled with thermodynamic modeling can therefore be used to calculate the strength of OPC-SCM systems (28, 29). Micromechanical modeling has also been used to predict the strength of cementitious systems by relating the strength to the porosity, pore volume distribution, and phase assemblage of these systems (30-33). While authors have attempted to extend these models to systems with limestone, Bentz et al. (34, 35) also examined the role of limestone on porosity and strength and DeLarrad (36) presented an approach that accounted for the acceleration and reaction effects of limestone fillers.

While the relationship between porosity and strength is well established, concrete's transport properties can also be related to the microstructure of concrete through the formation factor (F) (37-42). The formation factor is a microstructural property of a porous material related to the material's porosity and pore connectivity (43). Previous work has linked the formation factor of concrete to the transport properties of concrete, such as its ionic diffusivity (37, 38, 44), water permeability (45, 46), and sorption (47, 48). The transport processes can be used to predict the time to corrosion (40, 42, 49, 50) or the freeze-thaw performance (23, 40). It is also well established that these properties are positively affected by the presence of SCMs in the mixtures (28, 29, 51,

52). While several reports have stated that in general limestone improves transport properties Barrett et al. (53) noted some inconsistencies in PLC systems. As such, the role of limestone on the porosity, pore volumes, and pore connectivity need to be studied in OPC-Limestone-SCM systems.

The calcium hydroxide (CH) and pore solution in concrete can be related to key durability issues. First, the CH content directly related to deicing salt damage with $CaCl_2$, and $MgCl_2$ salts are used (54-58). The CH also acts as a pH buffer for the pore solution and affects the resistance of concrete to steel corrosion initiation and propagation (59) and carbonation (13), and along with the pore solution pH, the CH content affects the resistance of concrete to aggregate-silica reaction (ASR) damage (51, 60, 61). Pozzolanic reactions of SCMs consume CH in the system due to the presence of reactive silica and alumina. In addition, the reduction of the clinker phase may dilute the pore solution. This study will examine how the CH and pore solution vary when a portion of clinker is replaced with limestone and SCMs.

In this work, the impact of partial replacement of clinker with limestone in OPC-SCM systems is studied using thermodynamic modeling for different clinker and SCM chemistries. First, the effect of clinker chemistry (clinker used to make Type I/III and II/V cement) on OPC-Limestone systems' performance is studied. Next, the impact of partial replacement of the OPC-Limestone binder with 100% amorphous silica and 100% amorphous alumina (ideal SCM materials) is studied. Next, replacing a portion of the OPC-Limestone binder with commercial SCMs like fly ash, metakaolin, and slag is studied. Conclusions are drawn based on the performance of these systems with respect to the total porosity, CH content, unreacted calcite content, and pH of the pore solution. Finally, recommendations are made on the direct replacement of a portion of the clinker with limestone in OPC-SCM systems.

RESEARCH SIGNIFICANCE

This paper examines the influence of cement clinker chemistry on PLC performance. Specifically, simulations were performed using clinkers typical of those used in the manufacture of Type I, II, III, and V cement. The first portion of this paper compares OPC and PLC systems made with clinkers typical of different cement types to determine the significance of clinker chemistry with respect to PLC performance. The second portion of the research examines the influence of 100% alumina and silica (ideal SCMs) in systems where the limestone content is increased to 30%. This is done to provide insight on general trends that could be expected with SCMs. The third phase extended the model to commercially available SCMs at typical replacement levels. The work discusses how replacing OPC with PLC may impact the concrete performance and specifications.

MODELING FRAMEWORK

Thermodynamic Modeling

The GEMS3K (62) software is used to perform thermodynamic modeling, and it is coupled with the CEMDATA thermodynamic database (8). Thermodynamic modeling is performed by calculating the phase assemblage at equilibrium, which minimizes the system's Gibbs Free Energy. The GEMS-CEMDATA framework has been used to calculate the volumes and compositions of solids, liquid, and gaseous products at thermodynamic equilibrium. The framework has been used previously to obtain the reaction product volumes and pore solution composition of OPC (21, 22) and OPC+SCM systems (63). While all phases are available to form in the GEMS-CEMDATA framework, in this work, siliceous hydrogarnet (24, 63, 64), hydrotalcite

(24), and carbonate-ettringite phases (10, 65, 66) are blocked from forming based on empirical evidence from the literature that these phases do not form in significant quantities in cementitious systems at typical temperatures (less than 60°C) in the time frames studied (<20 years).

Kinetic Models

Thermodynamic models calculate only the phase assemblage of the systems studied at equilibrium (i.e., the final phases). In practice, most cementitious systems do not reach thermodynamic equilibrium. Kinetic models, such as the Parrot-Killoh model for OPC-clinker (67) or the Modified Parrot-Killoh Model for clinker + SCM (68), are often used to predict the mass fraction of the clinker that reacts at a given age. Thermodynamic models are often coupled with kinetic models to predict the reaction products of cementitious systems at a given age. The literature has shown that the phase assemblage of cementitious systems depends on the amount of clinker, SCM, and limestone available to react (8), and the kinetics of dissolution of the three components of the systems studied (i.e., clinker, SCM, limestone) are essential to understand and described in the following sections

Modified Parrot Killoh Model for Clinker and SCM

The Modified Parrot Killoh (MPK) model (68, 69) is used to predict the mass fraction of the clinker phases (C_3S, C_2S, C_3A, C_4AF) and oxide phases in SCMs (SiO_2, Al_2O_3, CaO) that react at a given age. The main inputs to the MPK model are: (i) the chemical composition of the OPC-clinker and SCM used, (ii) the reactivity of the SCM (fraction of SCM that can react at equilibrium, usually the amorphous fraction of the SCM (69)), (iii) water-to-cementitious materials ratio

(w/cm), and (iv) the temperature of curing. Other inputs include the fineness of the cement and SCM used. Note that the fineness of the cement used in this study is kept constant as studying the impact of fineness is beyond the scope of this study.

The MPK model outputs are the degree of reaction of the clinker phases (C_3S, C_2S, C_3A, C_4AF) and pozzolanic oxide phases (SiO_2, Al_2O_3, CaO) as a function of time. The degree of reaction of each phase at a given time ($DOR_{ph}(t)$) is the fraction of the component that is available to react at that time. The dissolution of the minor oxide phases in the clinker (Na_2O, K_2O, MgO, SO_3) are scaled based on their distribution in the clinker phases obtained from the literature (70). The dissolution of alkali oxide phases from the SCM were scaled with the reactivity (DOR^*) of the SCM and the degree of reaction of the SCM. The degree of reaction of the system (DOR_{sys}) is the mass averaged degree of reaction of clinker and SCM oxide phases (C_3S, C_2S, C_3A, C_4AF, SiO_2, Al_2O_3, CaO). Note: While the MPK model has only been validated for silica fume and fly ash, the authors believe that it may be used in this work to model other commercial SCMs such as slag and metakaolin. The MPK kinetic model is limited in its ability to capture the effects of particle packing and phase-specific local kinetic effects that may dominate in some special OPC+SCM systems (68, 69).

Modeling the Dissolution of Limestone

The mass of limestone available to react is an essential input parameter to thermodynamic calculations, impacting the phase assemblage (8) and porosity (9, 15, 71) of these systems. In this work, the amount of $CaCO_3$ available to react at any given time is considered the total amount of $CaCO_3$ in the system. Crystalline calcium carbonate is capable of dissolving at ambient

temperature (14, 65, 72). The total volume and fineness of calcite also play only a role in the amount of calcium carbonate dissolved at equilibrium (73). It has also been observed that the solubility of limestone in the pore solution of typical OPC+SCM systems is high enough to saturate the solution with carbonates within a few hours (74, 75), and often the effects of limestone dissolution kinetics disappear after the first hour of mixing (76). Therefore, limestone dissolution is governed by the kinetics of product formation and not the rate at which limestone dissolves. In this work, since the thermodynamic calculations are performed at ages greater than one day (typically $DOR_{sys} > 30\%$), the entire mass of calcium carbonate is considered to be available to react at all times. The portion of the calcium carbonate that does not react simply reprecipitates in the output of the thermodynamic model as calcite (which we assume would be undissolved) (8). While some of the calcium carbonate can be encapsulated by reaction products rendering the rest of the calcite unable to react, it is assumed in this work that this does not occur to a significant degree in the systems studied as the limestone is fine and generally sufficient limestone remains in the system.

Pore Partitioning Model

Thermodynamic modeling calculates the total volume of water that remains in the system at a given age. As such, it is unable to differentiate the size of pores that the water occupies. Recently, thermodynamic models have been combined synergistically with concepts from the Powers-Brownyard model to determine the volume of gel pores and capillary pores in OPC (24) and OPC+SCM systems (25). This is called the "Pore Partitioning Model" and is used in this work to determine the volumes of the Powers-Brownyard phases: unhydrated binder (of volume fraction

v_{ub} in the hydrated paste), gel solids (v_{gs}), gel water (v_{gw}, water in pores less than 5 nm in diameter), capillary water (v_{cw}, pores between 5nm and a few microns in diameter in the paste), and chemical shrinkage (v_{cs}). The total porosity of the cementitious paste (ϕ_{paste}) is calculated as the sum of the gel pores, capillary pores, and pores due to chemical shrinkage, such that:

$$\phi_{paste} = v_{gw} + v_{cw} + v_{cs} \quad (1)$$

NUMERICAL INVESTIGATION

This work describes several thermodynamic calculations to provide insight into the effects of limestone addition to OPC-SCM systems:

(i) The impact of clinker chemistry is studied on the performance of cements that contain limestone (PLCs). Two cements, Cement A (intended to be representative of the clinker used to make ASTM Type I/III cement commercially and its composition is calculated as the mean composition of Type I and Type III cements from (77)), and Cement B (intended to be representative of the clinker used to make ASTM Type II/V cement commercially and its composition is calculated as the mean composition of Type II and Type V cements from (77); the clinker used to make this cement has a lower C_3A content than Cement A) are studied in systems where the cement contains varying amounts of limestone (limestone content in the cement varies from 0% to 30% by mass). This provides insight into the impact of calcium carbonate on the phase assemblage (such as ettringite, monosulfate, hemi/monocarbonates, and CH) and pore volumes of typical PLC systems.

(ii) The impact of the partial replacement of 0-30% of the OPC or PLC with 100% amorphous silica (SiO_2) and 100% amorphous alumina (Al_2O_3) is studied on the bulk properties of pastes. This provides insight on the impact of the main pozzolanic components in SCMs on the bulk properties of pastes made with PLCs and SCMs.

(iii) The impact of partial replacement of PLCs of different limestone contents (0-30%) with commercially available SCMs like fly ash (FA), metakaolin (MK), and, slag (SL). These SCMs are chosen to demonstrate the impact of SCM composition on the behavior of PLC systems.

The w/cm is held constant at 0.42 (note that the mass of 'cementitious materials' used in calculating the w/cm is the sum of masses of cement, SCM and limestone) and the simulations are performed at an age of 56-days (the degree of hydration, DOH, is calculated to be about 71%). The compositions of the simulated clinker and SCMs are listed in Table 1. The composition of cement A (intending to represent the clinker used to produce Type I/III cements in the US) and cement B (intending to represent the clinker used to produce Type II/V cements in the US) is calculated as the mean composition of the typical ASTM Type I/III and ASTM Type II/V cements obtained from a literature study of 363 cements (77). Limestone is considered in these simulations to be calcium carbonate. Note that if the limestone is not pure, the total mass of $CaCO_3$ present in the limestone should be considered as limestone that is reported. The compositions of the fly ash and slag are based on the statistically average compositions of the SCMs obtained from the literature (78). The maximum degree of reaction (DOR*) values are chosen based on the typical reactivity of these materials observed in the lab (fly ash typically has a DOR* between 20% and 60%, MK has a DOR* between 55% and 100%, and slag typically has a DOR* between 25% and 75%, calculated from the pozzolanic reactivity test data available in the literature (79)).

RESULTS AND DISCUSSION

Influence of Limestone on Performance With Cements Having Two C_3A Contents

Figure 1 (a) and (b) show the predicted phase assemblage of cement pastes made with cement A (higher C_3A; intending to represent the clinker used to produce Type I/III cements in the US) and cement B (lower C_3A; intending to represent the clinker used to produce Type II/V cements in the US)) with increasing limestone contents in the binder. In both systems, the model predicts that as the limestone content is increased from 0% to 2%, hemicarbonates and monocarbonates form at the expense of monosulfates, which is consistent with the literature (8, 9, 15). Ettringite is also predicted to be stable when limestone is present in the system (8, 9). As the limestone content is increased beyond 3%, the modelling indicates that the volumes of major hydrate phases (calcium silicate hydrate or C-S-H, CH, hemi-/monocarbonate and ettringite) slightly decrease due to the dilution of clinker with limestone. Slightly more ettringite and hemi-/monocarbonate phases (~2% by volume) are predicted to be produced when clinker used to make Type I/III cements (cement A) is used when compared to clinker used to make Type II/V cements (cement B) due to a higher reacted aluminate from the clinker (see Table 1).

Figure 2 (a) and (b) show the predicted hydration products that form for cement pastes made with cements A and B with increasing limestone contents. Figure 2 (c) shows the predicted porosity of both systems as the limestone content increases. From Figure 2 (a) and Figure 2 (b), it can be seen that as the limestone content is increased from 0% (no limestone) to 2%, the predicted volume of gel solids increases by approximately 5%, and the predicted volume of capillary water decreases by approximately 4%. The model predicts the minimum porosity occurs at approximately 2% limestone by mass (Figure 2 (c)), consistent with the observations of Matschei

et al. (15). This is due to the formation of more "space-filling" phases (8, 9, 11), e.g., ettringite and hemi/monocarbonate form instead of monosulfates. This also leads to a reduction in the total porosity. The model predicts that the amount of gel water between a 0% and 2% limestone content remains nearly constant as the total volume of the phases that contribute to gel-water (monosulfate + ettringite + C-S-H) remain nearly constant. This leads to a lower predicted porosity of the gel phase between a 0% and 2% limestone content. The reduction in the predicted porosity of the gel phase is due to the formation of reaction products in the hydrated cement gel with lower porosity (carboaluminates) at the expense of higher porosity phases like monosulfates below a 2% limestone content.

For the reader's reference, a study of 68 commercial cements from North America showed that the average limestone contents in OPCs that contain limestone as an added ingredient is 3.1% (80). For both cements, the model predicts that above about 3% to 4% limestone content any additional limestone present in the system generally does not react. This causes a reduction in the volumes of gel solids and gel water due to dilution of reactive clinker with unreacted limestone. Despite the slightly different volumes of reaction products that form when cements with different C_3A contents are used, there is no significant difference in the predicted volumes of gel solids, gel water, or capillary water in the systems (each of these values are within 1% vol. fraction for both clinkers). This translates to nearly identical predicted total porosity for either system at a given limestone content, which can be seen in Figure 2 (c). Note that if the purity of the limestone is lower than 100%, the location of the point of minimum porosity shifts to a higher limestone content in a roughly linear manner (e.g., if the limestone is 100% calcite, the minimum porosity occurs at 2% limestone, and if the limestone only contains 50% $CaCO_3$, the minimum porosity would occur at around 4% limestone content).

Influence of Silica and Alumina on the Performance Properties of PLC systems

Porosity

Figure 3 (a) and (b) are plots of the predicted total porosity (using the PPM) of cementitious pastes made with higher C_3A clinker, typical of that used to produce Type I/III cement (see cement A in Table 1) blended with increasing weight fractions of limestone, with 100% amorphous silica and 100% amorphous alumina added as 'ideal' SCM's. The w/cm is 0.42 and the simulations are shown at an age of 56-days to allow for a significant pozzolanic reaction.

Figure 3 (a) shows the impact of the replacement of a fraction of the PLC with 100% amorphous silica. An increase in the limestone content causes a sharp decrease in the predicted porosity when the limestone replacement is increased from 0% (no limestone) to 1-2%, due to the formation of space filling phases (e.g., ettringite). The modeling results indicate that an increase in limestone content beyond 1-2% causes an increase in the predicted porosity of the paste due to clinker dilution. As the silica content in the pastes is increased, the model predicts that the porosity remains nearly the same up to a replacement level of around 25%, which is greater than most practical ranges. This is due to the competing effects of (i) dilution of PLC with silica ($DOR_{clinker}$ is between 70% and 80% for the studied age and replacement levels, DOR_{silica} is between 40% and 50% at the studied age and replacement levels, even though the silica is 100% reactive due to kinetic effects, calculated with the MPK model), and, (ii) the pozzolanic reaction of the silica which decreases capillary porosity. Any additional added silica (above 25%) results in the formation of stratlingite, which causes a reduction in the predicted porosity.

Figure 3 (b) shows the impact of replacing a fraction of the PLC with 100% amorphous alumina. The model predicts that if no alumina is present, an increase in limestone from 0-2%

causes a decrease in porosity from 38% to 34%, and at higher limestone concentrations (>2%), the porosity increases due to dilution. The model predicts that when alumina is added, and as long as the CH is not depleted, the alumina can react with limestone to form carboaluminate phases. These carboaluminate reactions decrease porosity as hemi-/monocarbonates are formed instead of monosulfates, and the synergistic reactions between alumina and limestone occur up to a 'critical limestone content', which is the maximum amount of limestone that can react for a given alumina content. The model predicts this critical limestone content to be 0% limestone for 0% alumina added, 2% limestone for 5% alumina, 5% limestone for 7.5% alumina, and 10% limestone for 9% alumina. This forms a low porosity 'wrinkle' in the contour plot of predicted porosity. This synergistic effect between limestone and alumina is shown more clearly in Figure 3 (c), which plots the porosity of 0%, 2.5%, 5%, and 7.5% alumina systems against the limestone addition. It can be seen that the point of minimum porosity moves to higher limestone contents when alumina is present, and the minimum porosity also reduces. The minimum paste porosity is 28% and occurs at the critical limestone content of 4% and an alumina content of 7.5%. This reduction occurs primarily due to the perfect balance of carbonates and alumina in the system, which results in the maximum amount of carboaluminate and ettringite phases forming (nearly 28% of the total volume is occupied by hemi-/monocarbonate phases and 8.5% by ettringite). If the alumina content is increased above 7.5%, even if limestone is available to react, the predicted porosity increases as there is an insufficient amount of sulfate to form ettringite. Instead, in this region ($7.5\%<Al_2O_3<9\%$ and $4\%<Ls<10\%$) more monosulfate forms rather than space-filling ettringite. At alumina concentrations >9%, the calcium hydroxide is depleted and stratlingite forms instead of monocarbonates, and the predicted porosity decreases (16). The minimum paste porosity occurs when alumina>9% is 26% and occurs at a limestone content of 10% and an alumina content of

30%. At all alumina levels, above the critical limestone content, the predicted porosity increases due to dilution.

Unreacted Calcite

Figure 4 (a) is a plot of the mass of unreacted calcite in the PLC + silica system obtained from thermodynamic modeling. First, it should be remembered our limestone is 100% calcite. For low levels of limestone addition (up to 2%) all of the limestone reacts. This is due to the initial reaction of limestone with the aluminate-containing clinker phases. As the limestone content increases (above a 2% limestone content), the model predictions show that the alumina appears to be reacted entirely (in this system, the only source of alumina is the cement), and there are no other phases available to react with the limestone. At high silica contents, a relatively negligible impact is observed on the amount of limestone that reacts (due to competing effects of dilution and filler effect).

Figure 4 (b) is a plot of the mass of unreacted calcite in the PLC - alumina system obtained from the thermodynamic model. As the amount of alumina in the system increases, the amount of limestone that can react also increases, consistent with what is expected in the literature (11). This can be seen as all of the unreacted calcite moving in a bilinear fashion with alumina additions of below 10% alumina having the amount of calcite remaining being directly is proportional to the amount of alumina added. When the alumina content is greater than 10%, the consumption of calcite is independent of the addition of more alumina (the maximum consumption of calcite appears to be 10% by mass irrespective of the amount of alumina added. This reaction limitation can be explained as follows. When the alumina content is below 10%, as the amount of limestone is increased, the model predicts that the calcite in the limestone reacts with the alumina and CH to

form hemicarbonates and monocarbonates. When the alumina content is greater than 10%, the model predicts that complete consumption of CH can occur (see Figure 5) leading to the remaining alumina being preferentially bound in phases like stratlingite (16). The beneficial effects of using SCMs containing a significant amount of alumina when PLCs are used is evident from these plots.

Calcium Hydroxide (CH) Content

Figure 5 (a) and (b) show the CH content of pastes made with PLC and silica/alumina as predicted by the thermodynamic model. In both cases, the model predicts that an increase in the addition of silica or alumina causes a decrease in CH due to the pozzolanic reactions. The alumina-based pozzolanic reaction consumes about twice the amount of CH (at the same SCM replacement level) as the silica-pozzolanic reaction. In the silica system, the model predicts that CH is depleted at a 20% silica content, and in the alumina system, the model predicts that CH is depleted at a 10% alumina content. Note that thermodynamic models cannot account for CH that is not available to react; therefore, it is possible to have some disparity between experimental and modelling results. It is likely that when the CH content in the paste is low, physical availability and kinetic effects dominate, and there will be some measurable CH in the system that is not available to participate in reactions (29, 55). This observation is consistent with literature where the CH content in pastes containing silica fume and limestone are compared to pastes containing metakaolin and limestone (16, 81). As the limestone content in the systems are increased from 0% to 2%, CH content slightly decreases and the increases due to the formation of hemicarbonates and subsequently monocarbonates. Any further increase in the limestone causes the CH content to steadily decrease due to dilution of the clinker (CH in these systems is produced due to clinker hydration).

Pore Solution pH

Figure 6 (a) and (b) are plots of the pH of the pore solution of pastes made with PLCs and silica or alumina as predicted by the thermodynamic model. In Figure 6 (a), as the silica content of the pastes is increased, the model predicts that the pore solution pH decreases due to the increased alkali binding and lower initial alkali in pore solution (due to dilution of clinker). Beyond a 20% silica addition by mass, the predicted pH drops rapidly due to the complete consumption of CH. As the limestone content is increased (up to approximately 2%), the predicted pH slightly increases (due to a reduction in solution volume). When the limestone is greater than approximately 2% the pH decreases due to the initial slight decrease in capillary water (which increases the concentration of hydroxyl ions in solution) and then subsequent dilution of clinker with limestone. In Figure 6 (b), as the alumina content of the pastes is increased, the predicted pH increases due to the reduction in the amount of C-S-H and the formation of stratlingite (stratlingite does not bind Na^+ and K^+ in the model used). As the limestone content in the pastes is increased, the predicted pH slightly increases and then decreases due to the initial slight decrease in the predicted volume of capillary water (which increases the concentration of hydroxyl ions in solution) and then subsequent dilution of clinker with limestone. This behavior is consistent with experimental observations (82).

Influence of Commercial SCMs on Performance Properties of PLC systems

The third part of this work is to study the impact of the addition of commercial SCMs like fly ash, metakaolin, and slag on the performance of cement+limestone systems. Simulations are

run from limestone fractions of 0% to 30%. The replacement of the cement+limestone binder with commercial SCMs is studied from 0% to 50% replacement by mass.

Fly Ash

Figure 7 contains plots of several performance properties of cementitious pastes made with varying weight fractions of limestone and fly ash (FA). Figure 7 (a) is a plot of the predicted porosity of the hydrated cement paste. As the amount of FA in the system increases, the predicted porosity uniformly increases due to dilution, as seen in experiments (29). When no FA is present, as the limestone content of the PLC increases from 0% to 2%, the predicted porosity initially decreases from 39% to 34% due to the formation of ettringite and monocarbonate, and if the limestone is increased above approximately 2% the predicted porosity increases due to dilution. When FA is present, the model predicts that the point of minimum porosity increases to higher limestone contents as the alumina in the FA can react with the calcite. This limestone content for minimum porosity is 2% when no FA is present, 3% for a 20% FA content, and 4-5% for a 40% FA content. These predicted trends reflect the near perfect balance of silica and alumina present in fly ash to synergistically react with calcite (limestone) to reduce the porosity.

Figure 7 (b) is a plot of the unreacted calcite present in the paste. The model predicts that as the amount of FA in the paste increases, the amount of reactive aluminate increases, and hence the amount of reacted calcite increases (and amount of unreacted calcite decreases). The model predicts that the unreacted calcite content follows a bilinear curve, with the unreacted calcite being zero up to the critical limestone content of 2% when no FA is present, 3% at a FA content of 20% and 4-5% for FA contents of 40% and above. Above a FA content of 40%, the maximum amount of limestone that can react as predicted by the model is 5% as the CH is depleted. Above the critical limestone content, the unreacted calcite is equal to the difference amount of calcite added and the

critical limestone content at that FA content. The model predicts that the amount of unreacted calcite increases proportional to the limestone content in the PLC.

Figure 7 (c) is a plot of the predicted CH content in the paste. The model predicts that as the amount of FA in the paste increases, the CH in the paste decreases due to the pozzolanic reactions. The model predicts that for the FA studied, the CH is completely depleted at a FA content of 40%. An increase in the limestone content of the PLC slightly decreases the CH due to the dilution of clinker (approximately 1.5g/100g_{binder} lower CH for a 10% increase in limestone).

Figure 7 (d) is a plot of the predicted pore solution pH in the system. As the amount of FA in the paste increases, the predicted pore solution pH decreases due to an increase in the amounts of alkali binding (more C-S-H is formed with a lower C/S). The model results indicate that an increase in the limestone content of the PLC slightly decreases the pH due to the dilution of clinker (lower mass of clinker translates to a lower mass of alkalis released into the pore solution).

Metakaolin

Figure 8 contains plots of several performance properties of cementitious pastes made with varying weight fractions of limestone and metakaolin (MK). Figure 8 (a) is a plot of the predicted porosity of the paste. As MK contains a significant fraction of reactive alumina, the model predicts that it is able to react with the limestone and cause a decrease in porosity when CH is present in the system (e.g. the point of minimum porosity, called “critical limestone content”, when no MK is present is 2% limestone, and when 15% MK is present is 4% limestone). Below a 15% MK content, if the limestone is increased beyond the critical limestone content, the predicted porosity increases due to dilution. Above a 15% MK content, thermodynamic modeling predicts that the

system runs out of CH and stratlingite forms rather than carboaluminate phases (formation of hemi/monocarbonates from alumina requires the presence of CH (16)), which cause a decrease in porosity as the MK content is increased. The minimum porosity in this region is 24% and occurs at 10% limestone + 40%MK. While this may improve mechanical properties and transport properties by greatly reducing the porosity, there is no CH to buffer against carbonation and corrosion. When MK>15%, the point of minimum porosity remains at 10% limestone content irrespective of the MK content, and any increase in the limestone content increases porosity due to dilution.

Figure 8 (b) is a plot of the unreacted calcite present in the paste obtained as the output of thermodynamic modeling. As the amount of MK in the paste increases, the model predicts that the amount of reacted calcite first increases and then decreases, which causes the amount of unreacted calcite to first decrease then increase. This appears to be due to reactions of the aluminate from the MK at lower replacement levels (MK<20%) with the carbonates in the limestone to form hemi-/monocarbonates. At higher replacement levels (MK>20%), the model predicts that as the amount of MK increases the amount of stratlingite increases in the system and it appears that the aluminate from the MK reacts with the silica present in the metakaolin in the absence of CH to form stratlingite (as it is unable to form hemi-/monocarbonates), which causes the amount of unreacted calcite to increase. The formation of stratlingite in OPC+Ls+MK pastes has been documented in the literature (16). As the amount of limestone in the PLC increases, the model predicts that all calcite that is able to react at a given MK replacement level reacts. Any additional calcite remains unreacted, and the amount of unreacted calcite increases proportional to the limestone content in the PLC.

Figure 8 (c) is a plot of the CH content in the paste as predicted from thermodynamic modeling. As the amount of MK in the paste increases, the predicted mass of CH in the paste decreases due to the pozzolanic reactions of the alumina and silica from the MK. The CH is completely depleted when MK>20%. The model shows that an increase in the limestone content of the PLC slightly decreases the CH due to the dilution of clinker (approximately 1.5g/100g_{binder} lower CH for a 10% increase in limestone).

Figure 8 (d) is a plot of the pore solution pH in the system, predicted using thermodynamic models. As the amount of MK in the paste increases, the predicted pH of the pore solution decreases due to an increase in the amounts of alkali binding (the model predicts that more C-S-H is formed with a lower C/S) and a decrease in the initial amounts of alkalis in the PLC+MK blend that go into solution. An increase in the limestone content of the PLC slightly decreases the predicted pH due to the dilution of clinker (lower mass of clinker translates to a lower mass of alkalis released into the pore solution).

Slag

Figure 9 contains plots of several predicted performance properties of cementitious pastes made with varying weight fractions of limestone and slag (SL). Figure 9 (a) is a plot of the predicted porosity of the paste. As the amount of SL in the system increases, the predicted porosity remains nearly constant due to the competing effects of (i) dilution, and, (ii) reactions between the CaO, SiO_2, and Al_2O_3 in the SL. When no SL is present, an increase in limestone from 0-2% causes the porosity to drop from 39% to 34%, and an increase in limestone above 2% causes an increase in porosity due to dilution. When SL is present, the model predicts that the alumina in the SL can react with the limestone in the presence of CH to produce carboaluminates and ettringite that

decrease the predicted porosity up to a critical limestone content. This critical limestone content as predicted by the model is 2% when no SL is present, 3.5% at a 25% SL content, and 5-6% at a 50% SL content. The minimum predicted porosity is 34-35% and occurs at the critical limestone content. The value of minimum porosity does not appear to be significantly affected by the SL content.

Figure 9 (b) is a plot of the predicted mass of unreacted calcite present in the paste. As the amount of SL in the paste increases, the amount of reactive aluminate increases and hence the model predicts that the amount of reacted calcite increases (and amount of unreacted calcite decreases). Since the addition of even 50% slag does not cause complete consumption of CH according to the model predictions, the reacted limestone increased with increasing slag content (up to 7.5% limestone reacts at a 50% slag content). The model also predicts that as the amount of limestone in the PLC increases, all calcite that is able to react at a given SL replacement level reacts. Any additional calcite remains unreacted, and the amount of unreacted calcite increases proportional to the limestone content in the PLC.

Figure 9 (c) is a plot of the predicted mass of CH present in the paste. As the amount of SL in the paste increases, the predicted mass of CH in the paste decreases due to the pozzolanic reactions. The model outputs show that this decrease is much lower than the decrease when FA or MK are used as the slag studied contains a significant portion of calcium that is able to react to form CH. An increase in the limestone content of the PLC has the following trend: (i) an initial decrease due to the formation of hemi-carbonates instead of C-A-H phases, (ii) a slight increase due to formation of monocarbonates rather than hemicarbonates as more carbonates are available to react in the system (notice that the point of minimum predicted porosity occurs in this same region), and, (iii) a decrease in the CH due to the dilution of clinker.

Figure 9 (d) is a plot of the predicted pore solution pH in the system. As the amount of SL in the paste increases, the predicted pH of the pore solution slightly decreases due to an increase in the amounts of alkali binding (more C-S-H is formed with a lower C/S). The model predicts that an increase in the limestone content of the PLC slightly decreases the pH due to the dilution of clinker (lower mass of clinker translates to a lower mass of alkalis released into the pore solution).

CONCLUSIONS

PLC (ASTM C595, Type IL) has been proposed as a direct replacement for OPC (ASTM C150). While ACI 318 and some state highway agencies permit the use of PLC after the 2012 revision of ASTM C595, some agencies have not adopted these cements yet. Questions have been raised on whether the clinker composition (clinkers used to make OPC Type I through V) or SCM use impacts the PLC's performance. This paper uses thermodynamic modeling to address these questions. A variety of limestone and SCM replacement levels in two types of clinker systems have been modeled to obtain properties of the hydrated systems such as porosity, pH, unreacted limestone (as calcite), and CH.

The use of cements with different C_3A contents (higher C_3A cements typical of ASTM Type I/III, and lower C_3A cements typical of Type II/V) to make PLC resulted in nearly identical porosity. For example, the porosity has been calculated as 38%, 34%, and 37% when 0%, 3%, and 15% by mass of limestone is respectively used to replace clinker. The reduction in porosity in PLC systems at low replacement levels appears to be due to the stabilization of ettringite and the formation of hemi/monocarbonate instead of monosulfate.

The performance of 'ideal' SCMs (100% alumina and 100% silica) is simulated for limestone contents between 0 and 30%. While thermodynamic models show that both the alumina and silica systems have reduced porosity, the porosity is shown to be lower in the system containing alumina due to the synergistic reactions between alumina and calcite to form hemi/monocarbonate phases when CH is available, and the formation of stratlingite when CH is depleted. Calcium hydroxide is reduced in both systems due to the pozzolanic reaction, as one may expect, irrespective of the limestone content.

The performance of PLCs is modeled with three typical commercially available SCMs: fly ash (FA), metakaolin (MK), and slag (SL) for various proportions. The decrease in the predicted porosity is most significant in PLC+MK due to the reactive alumina available. An increase in the amount of SCM in the PLC+FA system causes an increase in the estimated porosity, while an increase in the amount of SL in the PLC+SL system does not have a significant impact on the predicted porosity. The reduction in predicted mass of CH with increasing SCM replacement level is most significant in PLC+MK systems due to the higher pozzolanic reactivity. The model predicts that the decrease in CH is the least in PLC+SL systems due to the large amount of CaO available to react (hydraulically) in the slag. It is also found through modeling that the amount of calcite that reacts when CH is not depleted is roughly proportional to the mass of alumina that is available in the PLC+SCM systems. When CH is depleted, thermodynamic modeling predicts that stratlingite phases form as the formation of hemi/monocarbonate phases requires CH as a reactant.

In summary, SCM can be beneficially used with PLC. The model shows that alumina containing SCMs provide the most synergistic behavior when used with PLC systems. CH depletion would only occur at very high replacement levels and not those typically used in mixtures typically used in common building or state highway agency applications. As such, thermodynamic

modeling shows that PLCs can be used as a replacement for OPCs both without and with SCM. Future works include experimental work to validate the porosity and pore connectivity of pastes containing high volumes of limestone and SCMs. The current work also only looks at the mean compositions of the typical Type I/III cements (cement A) and Type II/V cements (cement B); future work will include a Monte-Carlo analysis of studying the variability of the compositions of these clinkers on the variation in the performance parameters of concrete made with PLCs and SCMs.

ACKNOWLEDGMENTS

The authors gratefully acknowledge the financial support provided by ARPA-E (Advanced Research Projects Agency-Energy), CALTRANS (California Department of Transportation), and National Science Foundation (Grant No. NSF CMMI 1728358). The authors gratefully acknowledge support from the John and Jean Loosely Chair and the Edwards Distinguished Chair at Oregon State, which have supported the last two authors respectively. The authors also acknowledge fruitful discussions with Prof. Barbara Lothenbach (EMPA, Switzerland).

REFERENCES

1. Tennis P, Thomas M, Weiss W, "State-of-the-Art Report on Use of Limestone in Cements at Levels of up to 15%," PCA R&D SN3148, Portland Cement Association, Skokie, IL. 2011.

2. Hawkins P, Tennis PD, Detwiler RJ, "The use of limestone in Portland cement: a state-of-the-art review." ENGINEERING BULLETIN 227: Portland Cement Association; 2005.

3. ASTM C150/C150M-19, " Standard Specification for Portland Cement," ASTM International, West Conshohocken, 2019.

4. AASHTO M85, " Standard Specification for Portland Cement," American Association of State Highway and Transportation Officials, Washington DC, 2020.

5. ASTM C595/C595M-20, " Standard Specification for Blended Hydraulic Cements," ASTM International, West Conshohocken, 2020.

6. AASHTO M240M/M240, " Standard Specification for Blended Hydraulic Cement," American Association of State Highway and Transportation Officials, Washington DC, 2020.

7. Hooton R, Thomas M, "Sulfate Resistance of Mortar and Concrete Produced with Portland-Limestone Cement and Supplementary Cementing Materials: Recommendation for ASTM C595/AASHTO M 240,", Portland Cement Association, Skokie, IL, USA, Report SN3285a, 2016.

8. Lothenbach B, Kulik DA, Matschei T, Balonis M, Baquerizo L, Dilnesa B, Miron GD, Myers RJ, "Cemdata 18: A chemical thermodynamic database for hydrated Portland cements and alkali-activated materials," Cement Concrete Res, V. 115, Jan. 2019, pp. 472-506.

9. Lothenbach B, Le Saout G, Gallucci E, Scrivener K, "Influence of limestone on the hydration of Portland cements," Cement Concrete Res, V. 38, No. 6. 2008, pp. 848-860.

10. Damidot D, Stronach S, Kindness A, Atkins M, Glasser F, "Thermodynamic investigation of the CaO Al_2O_3 $CaCO_3$ H_2O closed system at 25° C and the influence of Na_2O," Cement Concrete Res, V. 24, No. 3. 1994, pp. 563-572.

11. Ramezanianpour AM, Hooton RD, "A study on hydration, compressive strength, and porosity of Portland-limestone cement mixes containing SCMs," Cement and Concrete Composites, V. 51. 2014, pp. 1-13.

12. Thomas MD, Hooton RD, "The durability of concrete produced with portland-limestone cement: Canadian studies," PCA R&D SN3142, Portland Cement Association, Skokie, IL. 2010, 28 pp.

13. Matschei T, Glasser FP, "Temperature dependence, 0 to 40 C, of the mineralogy of Portland cement paste in the presence of calcium carbonate," Cement Concrete Res, V. 40, No. 5. 2010, pp. 763-777.

14. De Weerdt K, Kjellsen K, Sellevold E, Justnes H, "Synergy between fly ash and limestone powder in ternary cements," Cement and concrete composites, V. 33, No. 1. 2011, pp. 30-38.

15. Matschei T, Glasser FP, Herfort D, Lothenbach B, "Relationships of Cement Paste Mineralogy to Porosity and Mechanical Properties," International Conference on Modelling of Heterogeneous Materials with Applications in Construction and Biomedical Engineering, 2007.

16. Antoni M, Rossen J, Martirena F, Scrivener K, "Cement substitution by a combination of metakaolin and limestone," Cement Concrete Res, V. 42, No. 12. 2012, pp. 1579-1589.

17. Ashby MF, Cebon D, "Materials selection in mechanical design," MRS Bull, V. 30, No. 12. 2005, 995 pp.

18. Abrams DA, "Design of concrete mixtures, bulletin 1," Structural materials research laboratory Chicago: Lewis Institute. 1918.

19. Bolomey J, "Granulation et prévision de la résistance probable des bétons," Travaux, V. 19, No. 30. 1935, pp. 228-232.

20. Feret R, "On the compactness of the mortars," Annales des Ponts et Chaussées, Série, V. 7, No. 4, 1892, pp. 5-164.

21. Lothenbach B, Matschei T, Möschner G, Glasser FP, "Thermodynamic modelling of the effect of temperature on the hydration and porosity of Portland cement," Cement Concrete Res, V. 38, No. 1. 2008, pp. 1-18.

22. Lothenbach B, Winnefeld F, "Thermodynamic modelling of the hydration of Portland cement," Cement Concrete Res, V. 36, No. 2, Feb. 2006, pp. 209-226.

23. Bharadwaj K, Glosser D, Moradllo MK, Isgor OB, Weiss J, "Toward the Prediction of Pore Volumes and Freeze-Thaw Performance of Concrete Using Thermodynamic Modelling," Cement Concrete Res. V. 124, 2019, pp. 105820.

24. Azad VJ, Suraneni P, Isgor O, Weiss W, "Interpreting the pore structure of hydrating cement phases through a synergistic use of the Powers-Brownyard model, hydration kinetics, and thermodynamic calculations," Advances in Civil Engineering Materials, V. 6, No. 1. 2017, pp. 1-16.

25. Glosser D, Azad VJ, Suraneni P, Isgor B, Weiss J, "An extension of the Powers-Brownyard model to pastes containing SCM," ACI Materials Journal, V. 116, No. 5, 2019, pp. 205-216.

26. Powers TC, "Structure and physical properties of hardened Portland cement paste," Journal of the American Ceramic Society, V. 41, No. 1. 1958, pp. 1-6.

27. Powers TC, Brownyard TL, "Studies of the physical properties of hardened Portland cement paste," In Journal Proceedings, V. 43, No. 9, 1946, pp. 101-132.

28. Thomas M, "Supplementary cementing materials in concrete." CRC press; 2013.

29. Bharadwaj K, Ghantous RM, Sahan FN, Isgor BO, Weiss J, "Predicting Pore Volume, Compressive Strength, Pore Connectivity, and Formation Factor in Cementitious Pastes Containing Fly Ash," Cement and Concrete Composites, V. 122, 2021, pp. 104113.

30. Pichler B, Hellmich C, "Upscaling quasi-brittle strength of cement paste and mortar: A multi-scale engineering mechanics model," Cement Concrete Res, V. 41, No. 5, May. 2011, pp. 467-476.

31. Pichler B, Hellmich C, Eberhardsteiner J, Wasserbauer J, Termkhajornkit P, Barbarulo R, Chanvillard G, "The Counteracting Effects of Capillary Porosity and of Unhydrated Clinker Grains on the Macroscopic Strength of Hydrating Cement Paste–A Multiscale Model," Mechanics and Physics of Creep, Shrinkage, and Durability of Concrete: A Tribute to Zdeňk P Bažant, 2013, pp. 40-47.

32. Pichler B, Hellmich C, Eberhardsteiner J, Wasserbauer J, Termkhajornkit P, Barbarulo R, Chanvillard G, "Effect of gel-space ratio and microstructure on strength of hydrating cementitious materials: An engineering micromechanics approach," Cement Concrete Res, V. 45, Mar. 2013, pp. 55-68.

33. Termkhajornkit P, Vu QH, Barbarulo R, Daronnat S, Chanvillard G, "Dependence of compressive strength on phase assemblage in cement pastes: Beyond gel-space ratio - Experimental evidence and micromechanical modeling," Cement Concrete Res, V. 56, Feb. 2014, pp. 1-11.

34. Bentz DP, Ardani A, Barrett T, Jones SZ, Lootens D, Peltz MA, et al., "Multi-scale investigation of the performance of limestone in concrete," Construction and Building Materials, V. 75, 2015, pp. 1-10.

35. Bentz DP, Irassar EF, Bucher BE, Weiss WJ, "Limestone fillers conserve cement; Part 1: an analysis based on Powers' model," Concrete international, V. 31, No. 11. 2009, pp. 41-46.

36. de Larrad F, "Concrete mixture proportioning: a scientific approach. Modern Concrete Technology,", ed. A. Bentur und S, Mindess, 1999, 440 pp.

37. Snyder KA, "The relationship between the formation factor and the diffusion coefficient of porous materials saturated with concentrated electrolytes: theoretical and experimental considerations." 2000.

38. Spragg R, Qiao C, Barrett T, Weiss J, "Assessing a concrete's resistance to chloride ion ingress using the formation factor," Corrosion of steel in concrete structures, 2016, pp. 211-238.

39. Spragg R, Villani C, Weiss J, "Electrical properties of cementitious systems: formation factor determination and the influence of conditioning procedures," Advances in Civil Engineering Materials, V. 5, No. 1. 2016, pp. 124-148.

40. Weiss J, Ley MT, Isgor OB, Van Dam T, "Toward performance specifications for concrete durability: using the formation factor for corrosion and critical saturation for freeze-thaw," Proceedings of the 96th Annual Transportation Research Board, Washington, DC, USA. 2017, pp. 8-12.

41. Weiss WJ, Barrett TJ, Qiao C, Todak H, "Toward a specification for transport properties of concrete based on the formation factor of a sealed specimen," Advances in Civil Engineering Materials, V. 5, No. 1. 2016, pp. 179-194.

42. Weiss WJ, Spragg RP, Isgor OB, Ley MT, Van Dam T, "Toward performance specifications for concrete: linking resistivity, RCPT and diffusion predictions using the formation factor for use in specifications," High tech concrete: Where technology and engineering meet, Springer, 2018, pp. 2057-2065.

43. Archie GE, "The electrical resistivity log as an aid in determining some reservoir characteristics," Transactions of the AIME, V. 146, No. 01, 1942, pp. 54-62.

44. Qiao C, Coyle AT, Isgor OB, Weiss WJ, "Prediction of chloride ingress in saturated concrete using formation factor and chloride binding isotherm," Advances in Civil Engineering Materials, V. 7, No. 1, 2018, pp. 206-220.

45. Garboczi EJ, "Permeability, Diffusivity, and Microstructural Parameters - a Critical-Review," Cement Concrete Res, V. 20, No. 4, Jul. 1990, pp. 591-601.

46. Rajabipour F, "Insitu electrical sensing and material health monitoring in concrete structures," Ph.D. Thesis, Purdue University, West Lafayette, 2006.

47. Moradllo MK, Qiao C, Isgor B, Reese S, Weiss WJ, "Relating formation factor of concrete to water absorption," ACI Materials Journal, V. 115, No. 6, 2018, pp. 887-898.

48. Qiao C, Moradllo MK, Hall H, Ley MT, Weiss J, "Electrical Resistivity and Formation Factor of Air-Entrained Concrete," ACI Materials Journal, V. 116, No. 3, 2019.

49. Isgor OB, Weiss J, "A nearly self-sufficient framework for modelling reactive-transport processes in concrete," Materials and Structures, V. 52, No. 1, Feb. 2019.

50. Jafari Azad V, Erbektas AR, Qiao C, Isgor OB, Weiss WJ, "Relating the formation factor and chloride binding parameters to the apparent chloride diffusion coefficient of concrete," J Mater Civil Eng, V. 31, No. 2, 2019, pp. 04018392.

51. Lothenbach B, Scrivener K, Hooton RD, "Supplementary cementitious materials," Cement Concrete Res, V. 41, No. 12, Dec. 2011, pp. 1244-56.

52. Mehta PK, Monteiro PJ, "Concrete Microstructure, Properties and Materials," McGraw-Hill Education, 2006, 684 pp.

53. Barrett TJ, Sun H, Weiss WJ, "Performance of portland limestone cements: Cements designed to be more sustainable that include up to 15% limestone addition." 2013.

54. Monical J, Unal E, Barrett T, Farnam Y, Weiss WJ, "Reducing joint damage in concrete pavements: Quantifying calcium oxychloride formation," Transportation Research Record, V. 2577, No. 1, 2016, pp. 17-24.

55. Suraneni P, Azad VJ, Isgor BO, Weiss WJ, "Calcium oxychloride formation in pastes containing supplementary cementitious materials: Thoughts on the role of cement and supplementary cementitious materials reactivity," RILEM Technical Letters, V. 1, 2016, pp. 24-30.

56. Suraneni P, Monical J, Unal E, Farnam Y, Weiss J, "Calcium oxychloride formation potential in cementitious pastes exposed to blends of deicing salt," ACI Materials Journal, V. 114, No. 4, 2017, pp. 631-641.

57. Suraneni P, Salgado N, Carolan H, Li C, Azad V, Isgor B, Ideker J, Weiss WJ, "Mitigation of deicer damage in concrete pavements caused by calcium oxychloride formation–use of ground lightweight aggregates," International RILEM Conference on Materials, Systems and Structures in Civil Engineering, Lyngby, Denmark, 2016, pp. 171-180.

58. Whatley SN, Suraneni P, Azad VJ, Isgor OB, Weiss J, "Mitigation of calcium oxychloride formation in cement pastes using undensified silica fume," J Mater Civil Eng, V. 29, No. 10. 2017, pp. 04017198.

59. Ghods P, Isgor O, McRae G, Miller T, "The effect of concrete pore solution composition on the quality of passive oxide films on black steel reinforcement," Cement and Concrete Composites, V. 31, No. 1, 2009, pp. 2-11.

60. Hou X, Struble LJ, Kirkpatrick RJ, "Formation of ASR gel and the roles of CSH and portlandite," Cement Concrete Res, V. 34, No. 9, 2004, pp. 1683-1696.

61. Hooton R, Thomas M, Ramlochan T, "Use of pore solution analysis in design for concrete durability," Adv Cem Res, V. 22, No. 4, 2010, pp. 203-210.

62. Kulik DA, Wagner T, Dmytrieva SV, Kosakowski G, Hingerl FF, Chudnenko KV, et al., "GEM-Selektor geochemical modeling package: revised algorithm and GEMS3K numerical kernel for coupled simulation codes," Computational Geosciences, V. 17, No. 1, 2013, pp. 1-24.

63. Deschner F, Lothenbach B, Winnefeld F, Neubauer J, "Effect of temperature on the hydration of Portland cement blended with siliceous fly ash," Cement Concrete Res, V. 52, Oct. 2013, pp. 169-181.

64. Dilnesa BZ, Lothenbach B, Renaudin G, Wichser A, Kulik D, "Synthesis and characterization of hydrogarnet Ca3 (AlxFe1− x) 2 (SiO4) y (OH) 4 (3− y)," Cement Concrete Res, V. 59, 2014, pp. 96-111.

65. De Weerdt K, Haha MB, Le Saout G, Kjellsen KO, Justnes H, Lothenbach B, "Hydration mechanisms of ternary Portland cements containing limestone powder and fly ash," Cement Concrete Res, V. 41, No. 3, 2011, pp. 279-291.

66. Matschei T, Lothenbach B, Glasser FP, "Thermodynamic properties of Portland cement hydrates in the system CaO–Al2O3–SiO2–CaSO4–CaCO3–H2O," Cement Concrete Res, V. 37, No. 10, 2007, pp. 1379-1410.

67. Parrot LJ, "Prediction of cement hydration," Proceedings of the British Ceramic Society, 35, 1984, pp. 41-53.

68. Glosser D, Suraneni P, Isgor OB, Weiss WJ, "Estimating reaction kinetics of cementitious pastes containing fly ash," Cement and Concrete Composites, V. 112, 2020, pp. 103655.

69. Glosser DB, "Equilibrium and Non-equilibrium Thermodynamic Modeling of Cement Pastes Containing Supplementary Cementitious Materials," PhD Thesis, Oregon State University, Corvallis, 2020.

70. Taylor HF, "Cement chemistry." Thomas Telford London; 1997.

71. Choudhary A, Ghantous RM, Bharadwaj K, Opdahl O, Isgor OB, Weiss WJ, "Electrical and transport properties of cement mortar made using Portland Limestone Cement," Advances in Civil Engineering Materials, In Review, 2021..

72. Zajac M, Rossberg A, Le Saout G, Lothenbach B, "Influence of limestone and anhydrite on the hydration of Portland cements," Cement and Concrete Composites, V. 46, 2014, pp. 99-108.

73. Schöler A, Lothenbach B, Winnefeld F, Zajac M, "Hydration of quaternary Portland cement blends containing blast-furnace slag, siliceous fly ash and limestone powder," Cement and Concrete Composites, V. 55, 2015, pp. 374-382.

74. Zajac M, Dienemann W, Bolte G, "Comparative experimental and virtual investigations of the influence of calcium and magnesium carbonate on reacting cement," Proceedings of the 13th international congress on the chemistry of cements, Madrid, 2011.

75. Zajac M, Durdzinski P, Stabler C, Skocek J, Nied D, Haha MB, "Influence of calcium and magnesium carbonates on hydration kinetics, hydrate assemblage and microstructural development of metakaolin containing composite cements," Cement Concrete Res, V. 106, 2018, pp. 91-102.

76. Schöler A, Lothenbach B, Winnefeld F, Haha MB, Zajac M, Ludwig H-M, "Early hydration of SCM-blended Portland cements: A pore solution and isothermal calorimetry study," Cement Concrete Res, V. 93, 2017, pp. 71-82.

77. Bhatty, JI and Tennis, PD, U.S. and Canadian Cement Characteristics: 2004, SN2879, Portland Cement Association, 2008, 67 pp.

78. Azad VJ, Suraneni P, Trejo D, Weiss WJ, Isgor OB, "Thermodynamic investigation of allowable admixed chloride limits in concrete," ACI Materials Journal, V. 115, 2018, pp. 727-738.

79. Suraneni P, Hajibabaee A, Ramanathan S, Wang Y, Weiss J, "New insights from reactivity testing of supplementary cementitious materials," Cement and Concrete Composites, V. 103, 2019, pp. 331-338.

80. Tennis P, "Chemical and Physical Characteristics of US Hydraulic Cements: 2014," Portland Cement Association, Skokie, Ill. 2016.

81. Poon C-S, Lam L, Kou S, Wong Y-L, Wong R, "Rate of pozzolanic reaction of metakaolin in high-performance cement pastes," Cement Concrete Res, V. 31, No. 9, 2001, pp. 1301-1306.

82. Chopperla KST, Smith JA, Ideker J, "The efficacy of portland-limestone cements with supplementary cementitious materials to prevent alkali-silica reaction," Cement, In Review, 2021.

TABLES AND FIGURES

List of Tables:

List of Figures:

Figure 7 – Performance of cement+limestone and fly ash systems: (a) Porosity, (b) Unreacted Calcite, (c) Calcium Hydroxide Content, and, (d) Pore solution pH.

Figure 8 – Performance of cement+limestone and metakaolin systems: (a) Porosity, (b) Unreacted Calcite, (c) Calcium Hydroxide Content, and, (d) Pore solution pH.

Figure 9 – Performance of cement+limestone and slag systems: (a) Porosity, (b) Unreacted Calcite, (c) Calcium Hydroxide Content, and, (d) Pore solution pH.

Table 1. Compositions of cements and SCMs used in this study. All values are given in wt. %unless otherwise mentioned.

Constituent	Cement A (made with clinker used to produce Type I/III cements)	Cement B (made with clinker used to produce Type II/V cements)	Limestone (Ls)	Fly ash (FA)	Metakaolin (MK)	Slag (SL)
SiO_2	20.00	20.28	0	51.60	49.09	35.23
Al_2O_3	4.79	4.44	0	22.64	40.45	10.79
Fe_2O_3	2.95	3.50	0	8.89	1.45	0.86
CaO	63.31	63.63	0	7.55	0.16	38.65
Na_2O	0.16	0.16	0	1.06	0.09	0.31
K_2O	0.61	0.54	0	2.57	0.16	0.49
MgO	2.16	2.02	0	1.64	0.09	10.75
SO_3	3.52	2.94	0	0.73	0.04	1.52
$CaCO_3$	0	0	100	0	0	0
DOR*	-N/A-	- N/A-	- N/A-	40%	80%	60%
Specific Gravity	3.15	3.15	2.71	2.56	2.36	2.20
C_3S	57.91	59.13	- N/A-	- N/A-	- N/A-	- N/A-
C_2S	13.49	13.18	- N/A-	- N/A-	- N/A-	- N/A-
C_3A	7.68	5.82	- N/A-	- N/A-	- N/A-	- N/A-
C_4AF	8.90	10.63	- N/A-	- N/A-	- N/A-	- N/A-

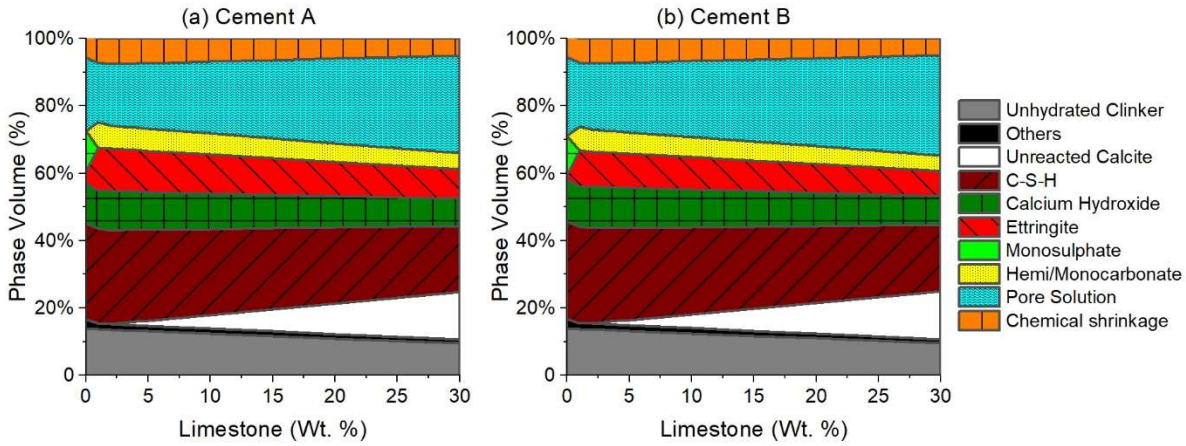

Figure 1. The model predicted Phase Assemblage of clinker + limestone systems made with (a) cement A (higher C_3A clinker, representative of clinkers used to produce Type I/III cement), and, (b) cement B (lower C_3A clinker, representative of clinkers used to produce Type II/V cement).

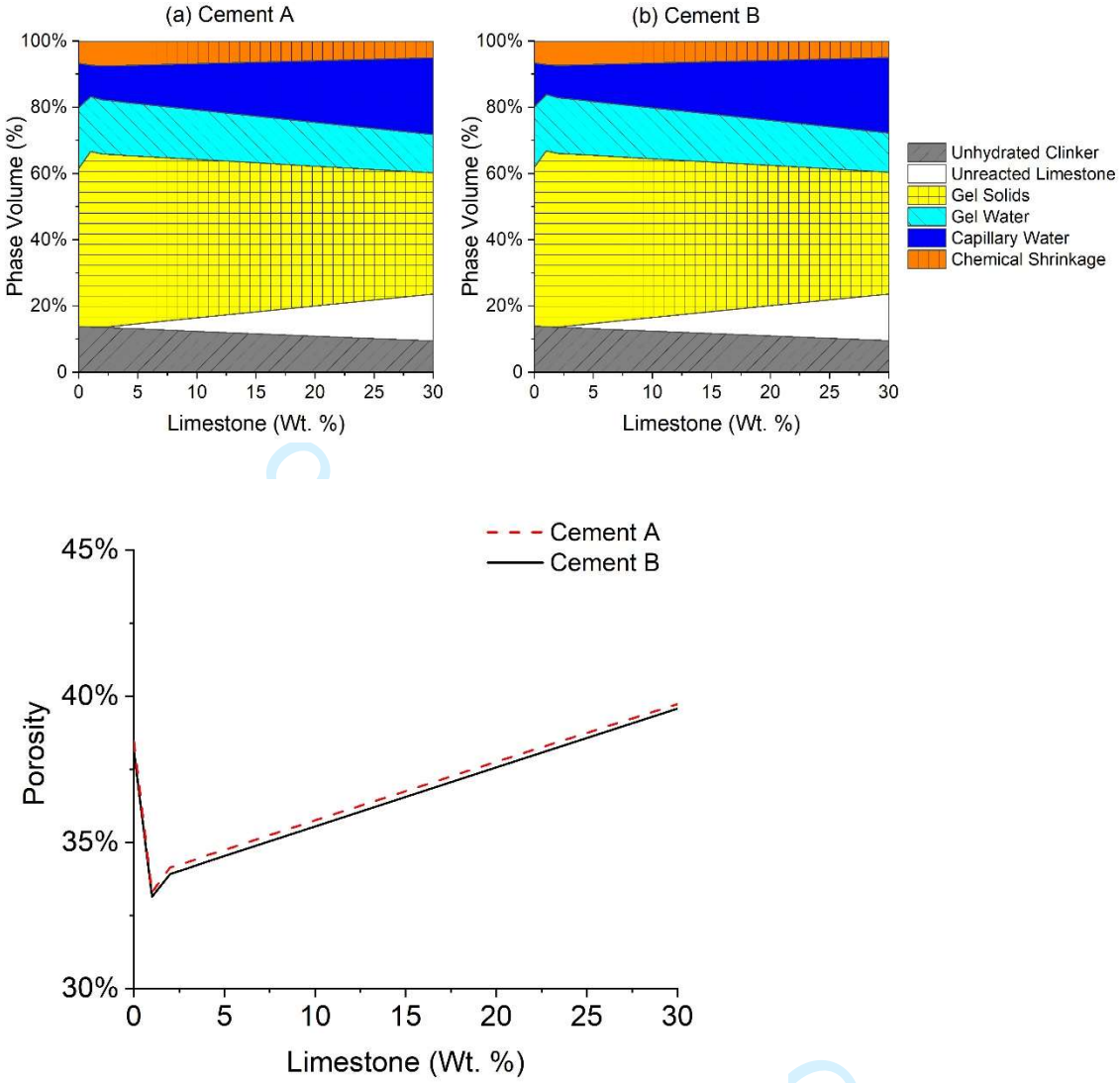

(c) Total Porosity of systems in (a) and (b).

Figure 2. Powers-Brownyard phases of clinker + limestone systems made with (a) cement A (higher C3A clinker, representative of clinkers used to produce Type I/III cement), and, (b) cement B (lower C3A clinker, representative of clinkers used to produce Type II/V cement); (c) Plot of total porosity of the PLC systems made with cement A and cement B.

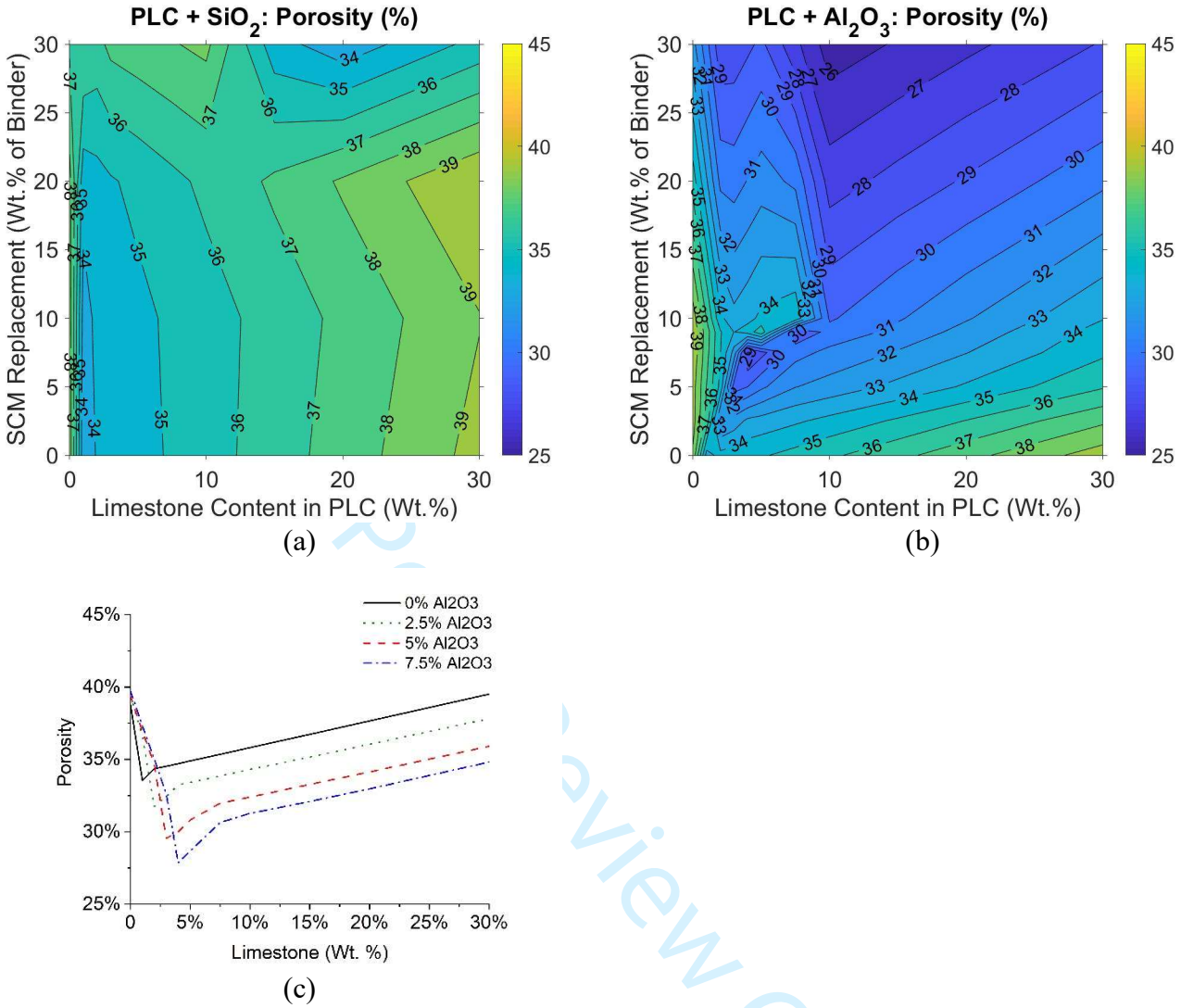

Figure 3. Total porosity of systems made with cement and varying levels of limestone for (a) 100% amorphous silica and (b) 100% amorphous alumina.

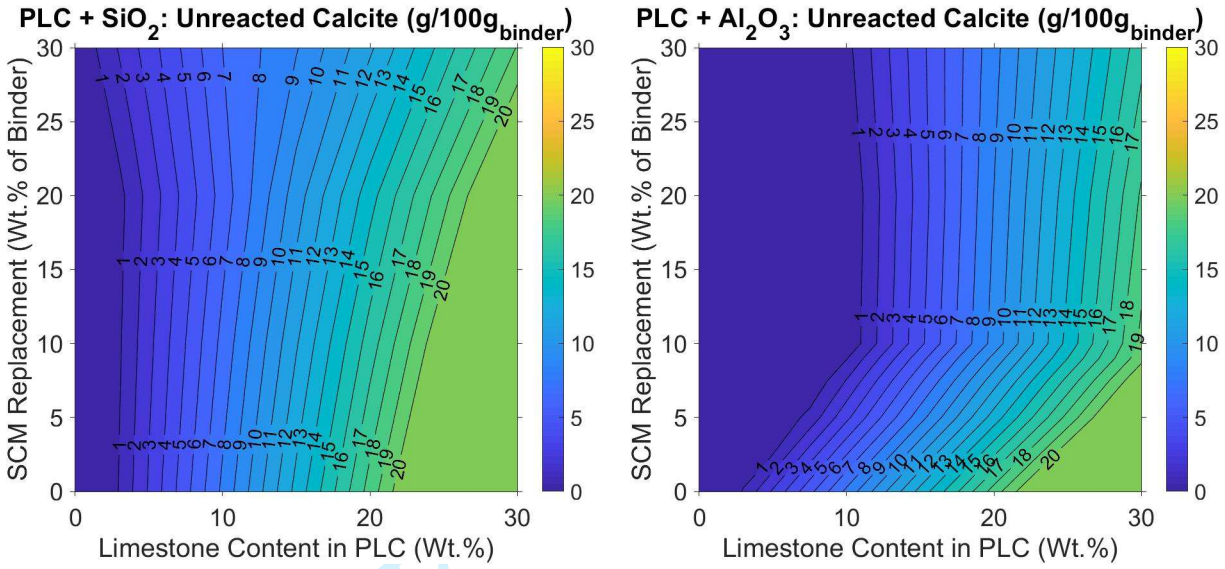

Figure 4. Unreacted calcite in systems made with cement and varying levels of limestone and (a) 100% amorphous silica, and, (b) 100% amorphous alumina.

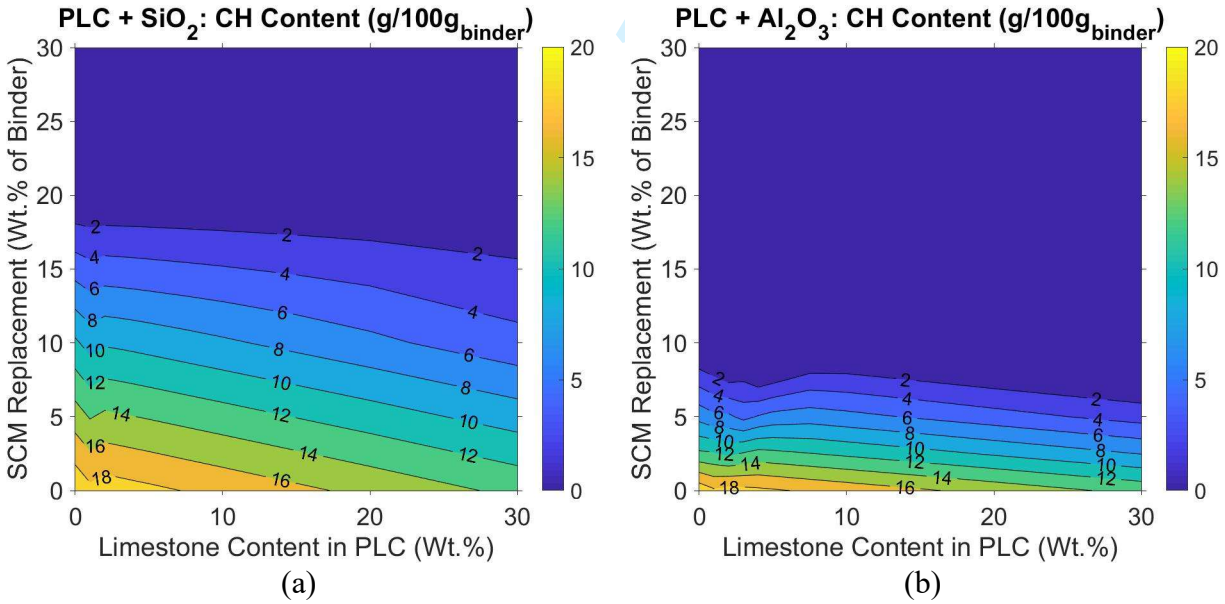

Figure 5. Calcium hydroxide mass in systems made with cement and varying levels of limestone and (a) 100% amorphous silica, and, (b) 100% amorphous alumina.

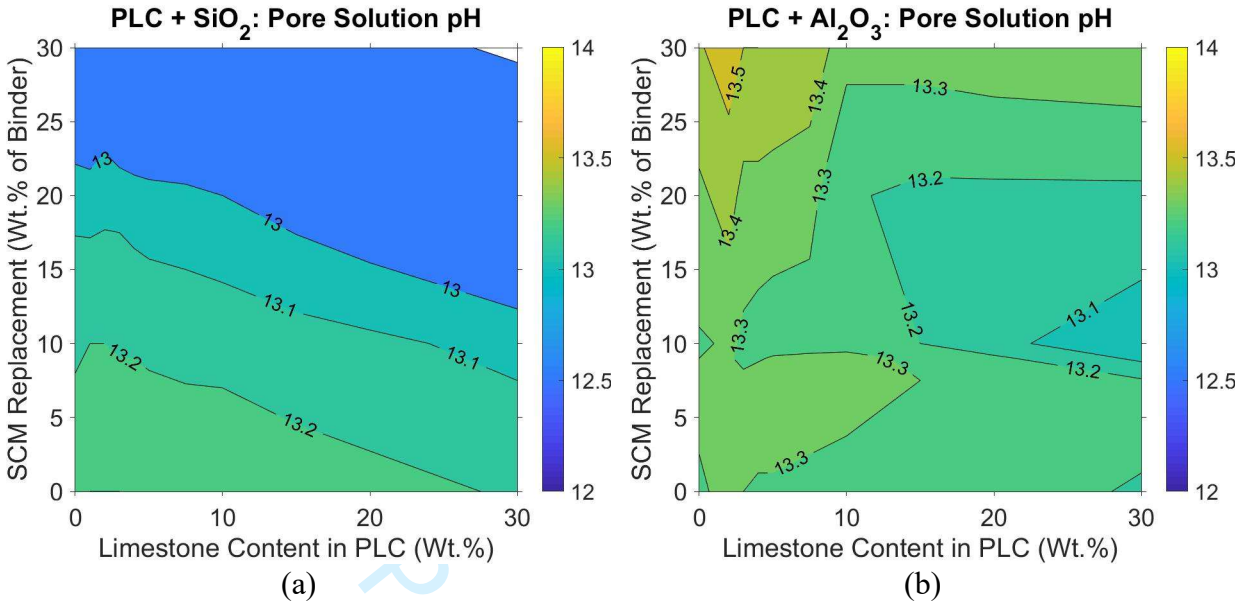

Figure 6. pH of the cement+limestone systems with: (a) 100% **amorphous silica, and, (b)** 100% **amorphous alumina.**

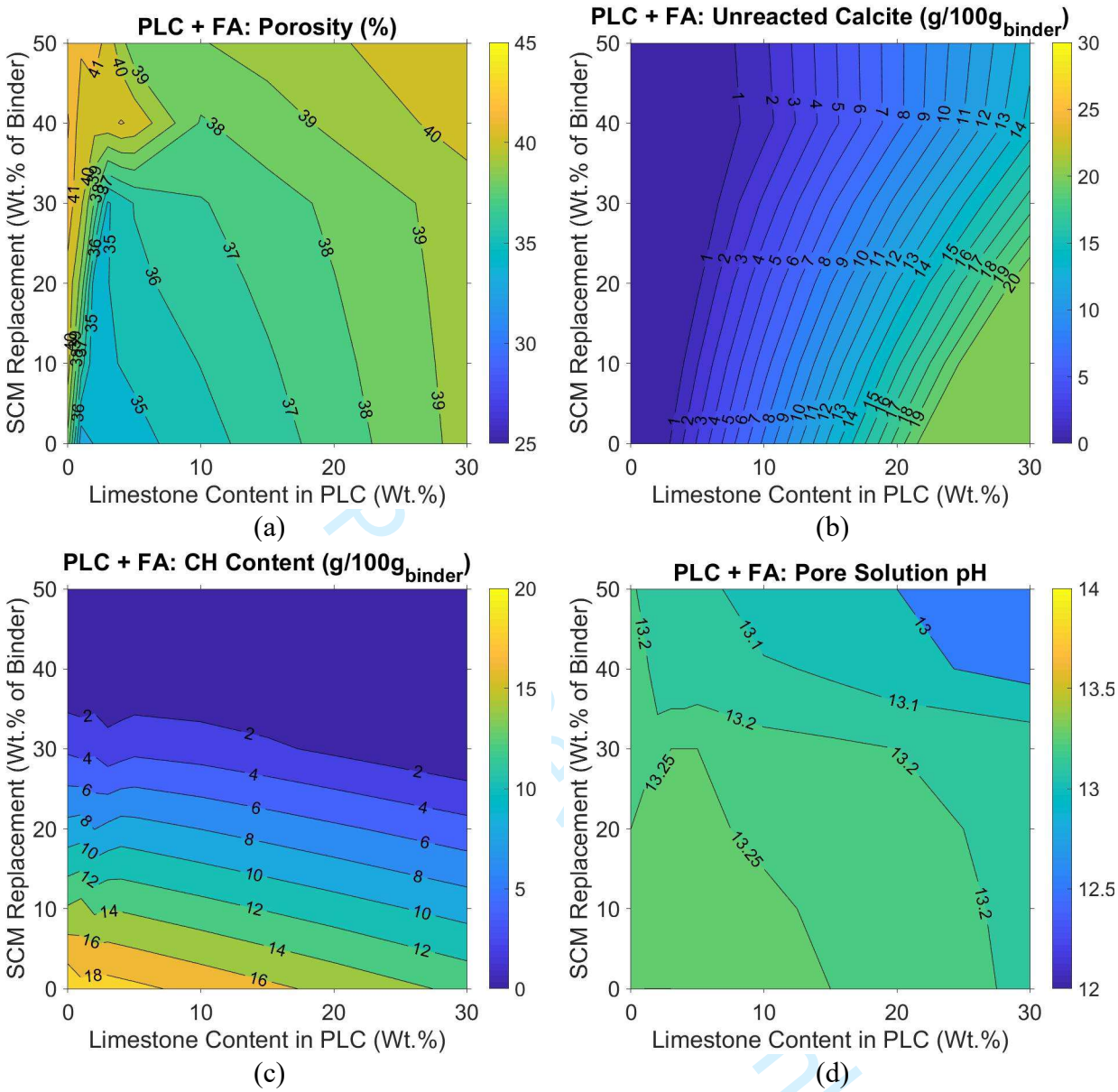

Figure 7. Performance of cement+limestone and fly ash systems: (a) Porosity, (b) Unreacted Calcite, (c) Calcium Hydroxide Content, and, (d) Pore solution pH.

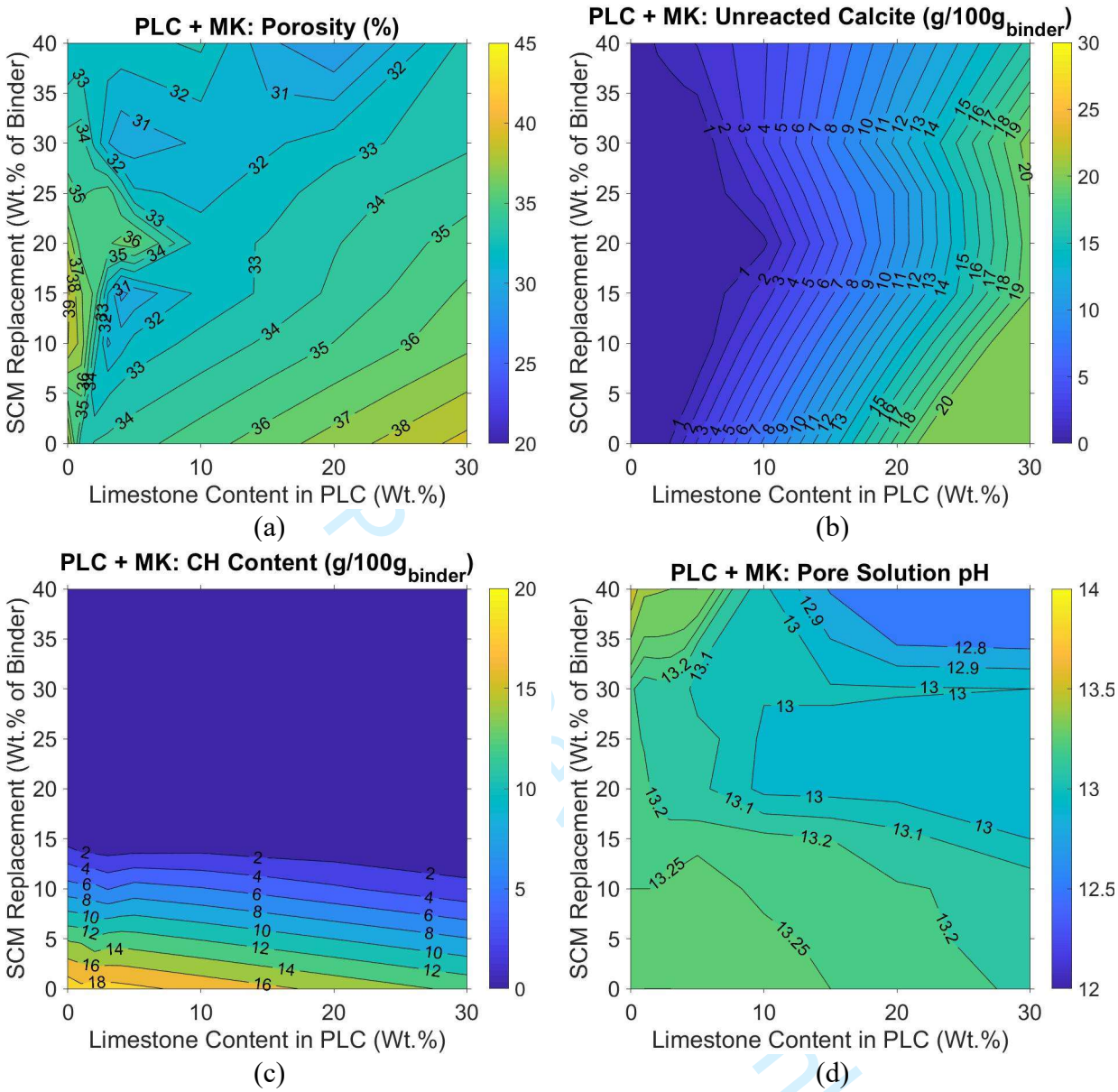

Figure 8. Performance of cement+limestone and metakaolin systems: (a) Porosity, (b) Unreacted Calcite, (c) Calcium Hydroxide Content, and, (d) Pore solution pH.

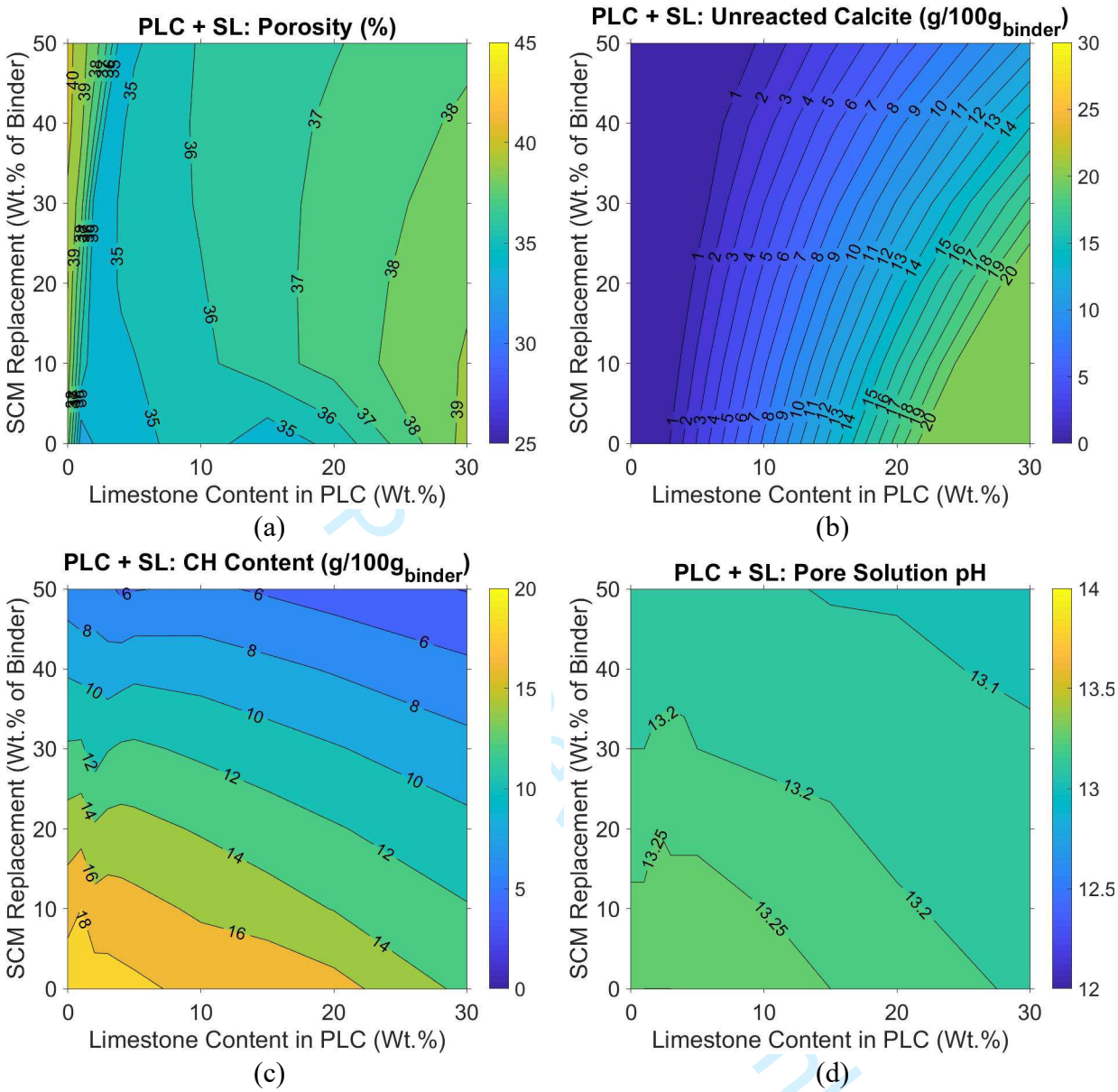

Figure 9. Performance of cement+limestone and slag systems: (a) Porosity, (b) Unreacted Calcite, (c) Calcium Hydroxide Content, and, (d) Pore solution pH.

Supplementary Cementitious Materials in Portland Limestone Cements

by Keshav Bharadwaj, O. Burkan Isgor, W. Jason Weiss

Biography:

ACI member **Keshav Bharadwaj** is a Ph.D. Student at Oregon State University, Corvallis, Oregon. He received his M.Tech. in Applied Mechanics and B.Tech. in Civil Engineering from the Indian Institute of Technology Madras, Chennai, India. His research interests include thermodynamic modeling, reactivity, transport in cementitious systems, and linking the microstructure of concrete to the engineering performance of concrete.

O. Burkan Isgor, FACI, is a professor in the School of Civil and Construction Engineering at Oregon State University, Corvallis, Oregon. He is the chair of ACI Committee 222, Corrosion of Metals in Concrete, and a member of ACI Committees 236, Material Science of Concrete, and 365, Service Life Prediction. His research interests include corrosion of steel in concrete, service-life modeling, and nondestructive testing.

Jason Weiss, FACI, is the Edwards Distinguished Professor of Engineering in the School of Civil and Construction Engineering at Oregon State University, Corvallis, Oregon. He is Editor in Chief of the ACI Materials Journal and a Member of the ACI Board.

ABSTRACT

Thermodynamic modeling was used to study the influence of ~~clinker (Type I/III and II/V)~~alumina in cements and supplementary cementing material (SCM) chemistry on the performance of ~~Portland~~ portland-~~L~~limestone ~~Cements~~ cements (PLC). ~~Clinker~~ The ~~Cement type~~ C_3A content of cement did not affect the porosity; however, ~~Type I/III clinkers,~~cements with ~~their~~ larger alumina content~~s~~, resulted in more ettringite formation than ~~Type II/V clinkers~~low alumina cements in systems with similar porosity. Alumina in clinker or SCM was ~~shown~~ predicted to ~~be reactive~~react with calcite to form hemi/monocarbonate phases when calcium hydroxide is available, and stratlingite ~~when~~ if calcium hydroxide is depleted. The decrease in the porosity was greater in the PLC+metakaolin systems due to the ~~reactive~~ higher available reactive alumina than PLC+fly ash and PLC+slag systems. SCMs can be beneficially used with PLC~~; however, care must be taken to ensure that calcium hydroxide is not entirely depleted.~~.

Keywords: Supplementary Cementitious Materials; Clinker; Limestone; Portland Limestone Cement; Thermodynamic modeling.

INTRODUCTION

The use of ~~Portland Limestone Cement~~ portland-limestone cements(PLC) as a replacement for ~~Ordinary~~ ordinary ~~Portland~~ portland ~~Cement~~ cement (OPC) in concrete has been gaining momentum due to inherent environmental benefits associated with the reduction of CO_2 emissions during production (1, 2). ASTM C150/ASHTO M85 typically allows up to 5% ground limestone content in OPCs (~~2~~ 3, 4), and ASTM C595/AASHTO M240 permits up to 15% limestone additions to the clinker (1, 5-7). Although some consider limestone an inert material, it can affect the reaction products of hydrated OPC systems (7-12). For example, in typical OPC systems, limestone content can stabilize ettringite and result in the formation of monocarbonate instead of monosulfate (8, 9, 12-14). This change in the phase assemblage of reaction products due to the presence of limestone can sometimes directly impact the porosity and pore volume distribution in concrete as ettringite is a more space-filling phase (1, 15). Matschei et al. (15) showed that the porosity of OPC-Limestone systems decreased (accompanied by an increase in compressive strength) when the limestone content increased from 0% to 2%, but any further increase in limestone content led to an increase in the porosity ~~increase~~ above the minimum porosity (and a decrease in compressive strength). It is worth noting that even at a 15% limestone content, the porosity of PLC systems is lower than the porosity of an OPC system with 0% limestone (15). Several authors have then experimentally studied the synergistic effect of using alumina containing supplementary ~~cementing~~ cementitious materials (SCMs) such as fly ash or metakaolin with limestone on the compressive strength of concrete (14, 16).

This work studies the impact of clinker chemistry and SCM addition on the reaction products and porosity of OPC-limestone systems. Concrete performance can be related to its porosity, pore volume distribution, and the chemical composition of its hydrated phases and pore

solution. Porosity is a key feature that can be related to engineering properties (17). For example, the strength of concrete made with OPC has been historically related to the water-to-~~binder~~ cement ratio (w/~~b~~c) through models such as Abram's model (18), Bolomey's model (19), or Feret's model (20). In these models, w/~~b~~ c was mainly used as a surrogate for the porosity of concrete. In recent years, Thermodynamic modeling has gained popularity as a tool to predict reaction products and porosity in cementitious systems (8, 21-23). Thermodynamic modeling has also been coupled with the Powers-Brownyard model to accurately calculate the porosity of pastes made of OPC (24) and OPC-SCM mixtures (25). ~~Powers and Brownyard's~~The Powers-Brownyard model accounts for pores of two sizes (gel and capillary) in OPC systems using the gel-to-space ratio to predict the compressive strength (26, 27). The Powers ~~and~~ -Brownyard approach coupled with thermodynamic modeling can therefore be used to calculate the strength of OPC-SCM systems (28, 29). Micromechanical modeling has also been used to predict the strength of cementitious systems by relating the strength to the porosity, pore volume distribution, and phase assemblage of these systems (30-33). While authors have attempted to extend these models to systems with limestone, Bentz et al. (34, 35) also examined the role of limestone on porosity and strength and DeLarrad (36) presented an approach that accounted for the acceleration and reaction effects of limestone fillers.

While the relationship between porosity and strength is well established, concrete's transport properties can also be related to the microstructure of concrete through the formation factor (F) (37-42). The formation factor is a microstructural property of a porous material related to the material's porosity and pore connectivity (43). Previous work has linked the formation factor of concrete to the transport properties of concrete, such as its ionic diffusivity (37, 38, 44), water permeability (45, 46), and sorption (47, 48). The transport processes can be used to predict the

time to corrosion (40, 42, 49, 50) or the freeze-thaw performance (23, 40). It is also well established that these properties are positively affected by the presence of SCMs in the mixtures (28, 29, 51, 52). While several reports have stated that in general limestone improves transport properties Barrett et al. (53) noted some inconsistencies in PLC systems. As such, the role of limestone on the porosity, ~~and~~ pore volumes, and pore connectivity need to be studied in OPC-Limestone-SCM systems.

The calcium hydroxide (CH) and pore solution in concrete can be related to key durability issues. First, the CH content directly related to deicing salt damage with $CaCl_2$, and $MgCl_2$ salts are used (54-58). The CH also acts as a pH buffer for the pore solution and affects the resistance of concrete to steel corrosion initiation and propagation (59) and carbonation (13), and along with the pore solution pH, the CH content affects the resistance of concrete to aggregate-silica reaction (ASR) damage (51, 60, 61). Pozzolanic reactions of SCMs consume CH in the system due to the presence of reactive silica and alumina. In addition, the reduction of the clinker phase may dilute the pore solution. This study will examine how the CH and pore solution vary when a portion of clinker is replaced with limestone and SCMs.

In this work, the impact of partial replacement of clinker with limestone in OPC-SCM systems is studied using thermodynamic modeling for different clinker and SCM chemistries. First, the effect of clinker chemistry (~~Type I/II and Type II/V clinkers~~clinker with lower C_3A content and clinker with higher C_3A content) on OPC-Limestone systems' performance is studied. Next, the impact of partial replacement of the OPC-Limestone binder with ~~pure~~ 100% amorphous silica and ~~pure~~ 100% amorphous alumina (ideal SCM materials) is studied. Next, replacing a portion of the OPC-Limestone binder with commercial SCMs like fly ash, metakaolin, and slag is studied. Conclusions are drawn based on the performance of these systems with respect to the total

porosity, ~~calcium hydroxide~~CH content, unreacted calcite content, and pH of the pore solution. Finally, recommendations are made on the direct replacement of a portion of the clinker with limestone in OPC-SCM systems.

RESEARCH SIGNIFICANCE

This paper examines the influence of cement clinker chemistry on PLC performance. Specifically, simulations were performed using clinkers typical of those used in the manufacture of Type I, II, III, and V cement. The first portion of this paper compares OPC and PLC systems made with clinkers typical of different cement types to determine the significance of clinker chemistry with respect to PLC performance. The second portion of the research examines the influence of ~~pure~~ 100% alumina and silica (ideal SCMs) in systems where the limestone content is increased to 30%. This is done to provide insight on general trends that could be expected with SCMs. The third phase extended the model to commercially available SCMs at typical replacement levels. The work discusses how replacing OPC with PLC may impact the concrete performance and specifications.

MODELING FRAMEWORK

Thermodynamic Modeling

The GEMS3K (62) software is used to perform thermodynamic modeling, and it is coupled with the CEMDATA thermodynamic database (8). Thermodynamic modeling is performed by calculating the phase assemblage at equilibrium, which minimizes the system's Gibbs Free

Energy. The GEMS-CEMDATA framework has been used to calculate the volumes and compositions of solids, liquid, and gaseous products at thermodynamic equilibrium. The framework has been used previously to obtain the reaction product volumes and pore solution composition of OPC (21, 22) and OPC+SCM systems (63). While all phases are available to form in the GEMS-CEMDATA framework, in this work, siliceous hydrogarnet (24, 63, 64), hydrotalcite (24), and carbonate-ettringite phases (10, 65, 66) are blocked from forming based on empirical evidence from the literature that these phases do not form in significant quantities in cementitious systems at typical temperatures (less than 60°C) in the time frames studied (<20 years).

Kinetic Models

Thermodynamic models calculate only the phase assemblage of the systems studied at equilibrium (i.e., the final phases). In practice, most cementitious systems do not reach thermodynamic equilibrium. Kinetic models, such as the Parrot-Killoh model for OPC-clinker (67) or the Modified Parrot-Killoh Model for clinker + SCM (68), are often used to predict the mass fraction of the clinker that reacts at a given age. Thermodynamic models are often coupled with kinetic models to predict the reaction products of cementitious systems at a given age. The literature has shown that the phase assemblage of cementitious systems depends on the amount of clinker, SCM, and limestone available to react (8), and the kinetics of dissolution of the three components of the systems studied (i.e., clinker, SCM, limestone) are essential to understand and described in the following sections

Modified Parrot Killoh Model for Clinker and SCM

The Modified Parrot Killoh (MPK) model (68, 69) is used to predict the mass fraction of the clinker phases (C_3S, C_2S, C_3A, C_4AF) and oxide phases in SCMs (SiO_2, Al_2O_3, CaO) that react at a given age. The main inputs to the MPK model are: (i) the chemical composition of the OPC-clinker and SCM used, (ii) the reactivity of the SCM (fraction of SCM that can react at equilibrium, usually the amorphous fraction of the SCM (69)), (iii) water-to-cementitious materials ratio (w/cm)~~w/b~~, and (iv) the temperature of curing. Other inputs include the fineness of the cement and SCM used. Note that the fineness of the cement used in this study is kept constant as studying the impact of fineness is beyond the scope of this study.

The MPK model outputs are the degree of reaction of the clinker phases (C_3S, C_2S, C_3A, C_4AF) and pozzolanic oxide phases (SiO_2, Al_2O_3, CaO) as a function of time. The degree of reaction of each phase at a given time ($DOR_{ph}(t)$) is the fraction of the component that is available to react at that time. The dissolution of the ~~alkali~~ minor oxide phases in the clinker (Na_2O, K_2O, MgO, SO_3) are scaled based on their distribution in the clinker phases obtained from the literature (70). The dissolution of alkali oxide phases from the SCM were scaled with the reactivity (DOR^*) of the SCM and the degree of reaction of the SCM. The degree of reaction of the system (DOR_{sys}) is the mass averaged degree of reaction of clinker and SCM oxide phases (C_3S, C_2S, C_3A, C_4AF, SiO_2, Al_2O_3, CaO). Note: While the MPK model has only been validated for ~~pure~~ silica fume and fly ash, the authors believe that it may be used in this work to model other commercial SCMs such as slag and metakaolin with reasonable accuracy. The MPK kinetic model is limited in its ability to capture the effects of particle packing and phase-specific local kinetic effects that may dominate in some special OPC+SCM systems (68, 69).

Modeling the Dissolution of Limestone

The mass of limestone available to react is an essential input parameter to thermodynamic calculations, impacting the phase assemblage (8) and porosity (9, 15, 71) of these systems. In this work, the amount of $CaCO_3$ available to react at any given time is considered the total amount of $CaCO_3$ in the system. Crystalline calcium carbonate is capable of dissolving at ambient temperature (14, 65, 72). The total volume and fineness of calcite also play only a role in the amount of calcium carbonate dissolved at equilibrium (73). It has also been observed that the solubility of limestone in the pore solution of typical OPC+SCM systems is high enough to saturate the solution with carbonates within a few hours (74, 75), and often the effects of limestone dissolution kinetics disappear after the first hour of mixing (76). Therefore, ~~the kinetics of~~ limestone dissolution is governed by the kinetics of product formation and not the rate at which limestone dissolves. In this work, since the thermodynamic calculations are performed at ages greater than one day (typically $DOR_{sys} > 30\%$), the entire mass of calcium carbonate is considered to be available to react at all times. The portion of the calcium carbonate that does not react simply reprecipitates in the output of the thermodynamic model as calcite (which we assume would be undissolved) (8). While some of the calcium carbonate can be encapsulated by reaction products rendering the rest of the calcite unable to react, it is assumed in this work that this does not occur to a significant degree in the systems studied as the limestone is fine and generally sufficient limestone remains in the system.

Pore Partitioning Model

Thermodynamic modeling calculates the total volume of water that remains in the system at a given age. As such, it is unable to differentiate the size of pores that the water occupies. Recently, thermodynamic models have been combined synergistically with concepts from the Powers-Brownyard model to determine the volume of gel pores and capillary pores in OPC (24) and OPC+SCM systems (25). This is called the "Pore Partitioning Model" and is used in this work to determine the volumes of the Powers-Brownyard phases: unhydrated binder (of volume fraction v_{ub} in the hydrated paste), gel solids (v_{gs}), gel water (v_{gw}, water in pores less than 5 nm in diameter), capillary water (v_{cw}, pores between 5nm and a few microns in diameter in the paste), and chemical shrinkage (v_{cs}). The total porosity of the cementitious paste (ϕ_{paste}) is calculated as the sum of the gel pores, capillary pores, and pores due to chemical shrinkage, such that:

$$\phi_{paste} = v_{gw} + v_{cw} + v_{cs} \quad (1)$$

NUMERICAL INVESTIGATION

This work describes several thermodynamic calculations to provide insight into the effects of limestone addition to OPC-SCM systems:

(i) The impact of clinker chemistry is studied on the performance of cements that contain limestone (PLCs). Two cements, Cement A (intended to be representative of the clinker used to make ASTM Type I/III cement commercially~~ASTM Type I/III~~ and the composition of this cement is calculated as the mean composition of Type I and Type III cements from (77); the clinker used to make this cement has a higher C_3A content), and Cement B (intended to be representative of the clinker used to make ASTM Type

II/V cement commercially ~~Type II/V clinkers~~ and the composition of this cement is calculated as the mean composition of Type II and Type V cements from (77); the clinker used to make this cement has a lower C_3A content) are studied in systems where the cement contains varying amounts of limestone (limestone content ~~replaces~~ in the cement varies from 0% to 30% ~~of the cement~~by mass). This provides insight into the impact of calcium carbonate on the phase assemblage (such as ettringite, monosulfate, hemi/monocarbonates, and CH) and pore volumes of typical PLC systems.

(ii) The impact of the partial replacement of 0-30% of the OPC or PLC with ~~pure~~ 100% amorphous silica (SiO_2) and ~~pure~~ 100% amorphous alumina (Al_2O_3) is studied on the bulk properties of pastes. This provides insight on the impact of the main pozzolanic components in SCMs on the bulk properties of pastes made with PLCs and SCMs.

(iii) The impact of partial replacement of PLCs of different limestone contents (0-30%) with commercially available SCMs like fly ash (FA), metakaolin (MK), and, slag (SL). These SCMs are chosen to demonstrate the impact of SCM composition on the behavior of PLC systems.

The w/~~b~~ cm is held constant at 0.42 (note that the mass of 'cementitious materials' used in calculating the w/cm is the sum of masses of cement, SCM and limestone) and the simulations are performed at an age of 56-days (the degree of hydration, DOH, is calculated to be about 71%). The compositions of the simulated clinker and SCMs are listed in Table 1. The ~~mean~~ composition of ~~ASTM Type I/III and ASTM Type II/V clinkers~~cement A (intending to represent the clinker used to produce Type I/III cements in the US) and cement B (intending to represent the clinker used to produce Type II/V cements in the US) is calculated as the mean composition of the typical ASTM Type I/III and ASTM Type II/V cements obtained from ~~based on~~ a literature study of 363

cements ~~is used~~ (77). Limestone is considered in these simulations to be ~~pure~~ calcium carbonate. Note that if the limestone is not pure, the total mass of $CaCO_3$ present in the limestone should be considered as limestone that is reported. The compositions of the fly ash and slag are based on the statistically average compositions of the SCMs obtained from the literature (78). The maximum degree of reaction (DOR*) values are chosen based on the typical reactivity of these materials observed in the lab (fly ash typically has a DOR* between 20% and 60%, MK has a DOR* between 55% and 100%, and slag typically has a DOR* between 25% and 75%, calculated from the pozzolanic reactivity test data available in the literature (79)).

RESULTS AND DISCUSSION

Influence of Limestone on Mixtures with ~~Type I/III and Type II/V Clinkers~~Cements with lower C_3A and higher C_3A

Figure 1 (a) and (b) show the predicted phase assemblage of cement pastes made with ~~Type I/III~~cement A (higher C_3A; intending to represent the clinker used to produce Type I/III cements in the US) and ~~Type II/V clinkers~~cement B (lower C_3A; intending to represent the clinker used to produce Type II/V cements in the US)) with increasing limestone contents in the binder. In both systems, the model predicts that as the limestone content is increased from 0% to 2%, hemicarbonates and monocarbonates form at the expense of monosulfates, which is consistent with the literature (8, 9, 15). Ettringite is also predicted to be stable~~ilized~~ when limestone is present in the system (8, 9). As the limestone content is increased beyond 3%, the modelling indicates that the volumes of major hydrate phases (calcium silicate hydrate or C-S-H, CH, hemi-/monocarbonate and ettringite) slightly decrease due to the dilution of clinker with limestone.

Slightly more ettringite and hemi-/monocarbonate phases (~2% by volume) are predicted to be produced when ~~Type I/III clinker~~clinker used to make Type I/III cements (cement A) is used when compared to ~~Type II/V clinker~~clinker used to make Type II/V cements (cement B) due to a higher reacted aluminate from the clinker (see Table 1).

Figure 2 (a) and (b) show the predicted hydration products that form for cement pastes made with ~~Type I/III and Type II/V clinker~~cements A and B with increasing limestone contents. Figure 2 (c) shows the predicted porosity of both systems as the limestone content increases. From Figure 2 (a) and Figure 2 (b), it can be seen that as the limestone content is increased from 0% (no limestone) to 2%, the predicted volume of gel solids increases by approximately 5%, and the predicted volume of capillary water decreases by approximately 4%. The model predicts the minimum porosity occurs at approximately 2% limestone by mass (Figure 2 (c)), consistent with the observations of Matschei et al. (15). This is due to the formation of more "space-filling" phases (8, 9, 11), ~~(~~e.g., ettringite and hemi/monocarbonate —form instead of monosulfates~~)~~. This also leads to a reduction in the total porosity. The model predicts that the amount of gel water between a 0% and 2% limestone content remains nearly constant as the total volume of the phases that contribute to gel-water (monosulfate + ettringite + C-S-H) remain nearly constant. This leads to a lower predicted porosity of the gel phase between a 0% and 2% limestone content. The reduction in the predicted porosity of the gel phase is due to the formation of reaction products in the hydrated cement gel with lower porosity (carboaluminates) at the expense of higher porosity phases like monosulfates below a 2% limestone content.

For the reader's reference, a study of 68 commercial cements from North America showed that the average limestone contents in OPCs that contain limestone as an added ingredient is 3.1% (80). For both ~~clinkers~~cements, the model predicts that above ~~a~~ about 3-% to 4% limestone content~~,~~

any additional limestone present in the system generally does not react. This causes a reduction in the volumes of gel solids and gel water due to dilution of reactive clinker with unreacted limestone. Despite the slightly different volumes of reaction products that form when ~~Type I/III clinkers and Type II/V clinkers~~cements with different C_3A contents are used, there is no significant difference in the predicted volumes of gel solids, gel water, or capillary water in the systems (each of these values are within 1% vol. fraction for both clinkers). This translates to nearly identical predicted total porosity for either system at a given limestone content, which can be seen in Figure 2 (c). Note that if the purity of the limestone is lower than 100%, the location of the point of minimum porosity shifts to a higher limestone content in a roughly linear manner (e.g., if the limestone is 100% calcite, the minimum porosity occurs at 2% limestone, and if the limestone only contains 50% $CaCO_3$, the minimum porosity would occur at around 4% limestone content).

Influence of ~~Pure~~ Silica and ~~Pure~~ Alumina on the Performance Properties of PLC systems

Porosity

Figure 3 (a) and (b) are plots of the predicted total porosity (using the PPM) of cementitious pastes made with ~~Type I/III clinker~~higher C_3A clinker, typical of that used to produce Type I/III cement (see cement A in Table 1) blended with increasing weight fractions of limestone, with ~~pure~~ 100% amorphous silica and ~~or~~ 100% amorphous alumina added as 'ideal' SCM's. The w/~~b~~ cm is 0.42 and the simulations are shown at an age of 56-days to allow for a significant pozzolanic reaction.

Figure 3 (a) shows the impact of the replacement of a fraction of the PLC with ~~pure~~ 100% amorphous silica. An increase in the limestone content causes a sharp decrease in the predicted

porosity when the limestone replacement is increased from 0% (no limestone) to 1-2%, due to the formation of space filling phases (e.g., ettringite). The modeling results indicate that ~~An~~ an increase in limestone content beyond 1-2% causes an increase in the predicted porosity of the paste due to clinker dilution. As the silica content in the pastes is increased, the model predicts that the porosity remains nearly the same up to a replacement level of around 25%, which is greater than most practical ranges. This is due to the competing effects of (i) dilution of PLC with silica ($DOR_{clinker}$ is between 70% and 80% for the studied age and replacement levels, DOR_{silica} is between 40% and 50% at the studied age and replacement levels, even though the silica is 100% reactive due to kinetic effects, calculated with the MPK model), and, (ii) the pozzolanic reaction of the silica which decreases capillary porosity. Any additional added silica (above 25%) results in the formation of stratlingite, which causes a reduction in the predicted porosity.

Figure 3 (b) shows the impact of replacing a fraction of the PLC with ~~pure~~ 100% amorphous alumina. The model predicts that ~~If~~ if no alumina is present, an increase in limestone from 0-2% causes a decrease in porosity from 38% to 34%, and at higher limestone concentrations (>2%), the porosity increases due to dilution. The model predicts that ~~When~~ when alumina is added, and as long as the CH is not depleted, the alumina can react with limestone to form carboaluminate phases. These carboaluminate reactions decrease porosity as hemi-/monocarbonates are formed instead of monosulfates, and the synergistic reactions between alumina and limestone occur up to a 'critical limestone content', which is the maximum amount of limestone that can react for a given alumina content. The model predicts this critical limestone content ~~is~~ to be 0% limestone for 0% alumina added, 2% limestone for 5% alumina, 5% limestone for 7.5% alumina, and 10% limestone for 9% alumina. This forms a low porosity 'wrinkle' in the contour plot of predicted porosity. This synergistic effect between limestone and alumina is shown

more clearly in Figure 3 (c), which plots the porosity of 0%, 2.5%, 5%, and 7.5% alumina systems against the limestone addition. It can be seen that the point of minimum porosity moves to higher limestone contents when alumina is present, and the minimum porosity also reduces. The minimum paste porosity is 28% and occurs at the critical limestone content of 4% and an alumina content of 7.5%. This reduction occurs primarily due to the perfect balance of carbonates and alumina in the system, which results in the maximum amount of carboaluminate and ettringite phases forming (nearly 28% of the total volume is occupied by hemi-/monocarbonate phases and 8.5% by ettringite). If the alumina content is increased above 7.5%, even if limestone is available to react, the predicted porosity increases as there is an insufficient amount of sulfate to form ettringite. Instead, in this region ($7.5\%<Al_2O_3<9\%$ and $4\%<Ls<10\%$) more monosulfate forms rather than space-filling ettringite. At alumina concentrations >9%, the calcium hydroxide is depleted and stratlingite forms instead of monocarbonates, and the predicted porosity decreases (16). The minimum paste porosity occurs when alumina>9% is 26% and occurs at a limestone content of 10% and an alumina content of 30%. At all alumina levels, above the critical limestone content, the predicted porosity increases due to dilution.

Unreacted Calcite

Figure 4 (a) is a plot of the mass of unreacted calcite in the PLC + silica system obtained from thermodynamic modeling. First, it should be remembered our limestone is 100% calcite. For low levels of limestone addition (up to 2%) all of the limestone reacts. This is due to the initial reaction of limestone with the aluminate-containing clinker phases. As the limestone content increases (above a 2% limestone content), the model predictions show that the alumina appears to be reacted entirely (in this system, the only source of alumina is the cement), and there are no other

phases available to react with the limestone. At high silica contents, a relatively negligible impact is observed on the amount of limestone that reacts (due to competing effects of dilution and filler effect).

Figure 4 (b) is a plot of the mass of unreacted calcite in the PLC - alumina system obtained from the thermodynamic models. As the amount of alumina in the system increases, the amount of limestone that can react also increases, consistent with what is expected in the literature (11). This can be seen as all of the unreacted calcite moving in a bilinear fashion with alumina additions of below 10% alumina having the amount of calcite remaining being directly is proportional to the amount of alumina added. When the alumina content is greater than 10%, the consumption of calcite is independent of the addition of more alumina (the maximum consumption of calcite appears to be 10% by mass irrespective of the amount of alumina added. This reaction limitation can be explained as follows. When the alumina content is below 10%, as the amount of limestone is increased, the model predicts that the calcite in the limestone reacts with the alumina and ~~calcium hydroxide~~CH to form hemicarbonates and monocarbonates. When the alumina content is greater than 10%, the model predicts that complete consumption of ~~calcium hydroxide~~CH can occur (see Figure 5) leading to the remaining alumina being preferentially bound in ~~C-(A)-S-H~~ phases ~~(~~like stratlingite~~)~~ (16). The beneficial effects of using SCMs containing a significant amount of alumina when PLCs are used is evident from these plots.

Calcium Hydroxide (CH) Content

Figure 5 (a) and (b) show the ~~calcium hydroxide~~CH content of pastes made with PLC and silica/alumina as predicted by the thermodynamic models. In both cases, the model predicts that an increase in the addition of silica or alumina causes a decrease in ~~the calcium hydroxide~~ CH due

to the pozzolanic reactions. The alumina-based pozzolanic reaction consumes about twice the amount of CH~~calcium hydroxide~~ (at the same SCM replacement level) as the silica-pozzolanic reaction. In the silica system, the model predicts that CH is depleted at a 20% silica content, and in the alumina system, the model predicts that CH is depleted at a 10% alumina content. Note that thermodynamic models cannot account for CH that is not available to react; therefore, it is possible to have some disparity between experimental and modelling results. It is likely that when the CH content in the paste is low, physical availability and kinetic effects dominate, and there will be some measurable CH in the system that is not available to participate in reactions (29, 55). This observation is consistent with literature where the ~~Calcium calcium~~CH ~~Hydroxide hydroxide~~ content in pastes containing silica fume and limestone are compared to pastes containing metakaolin and limestone (16, 81). As the limestone content in the systems are increased from 0% to 2%, CH content ~~the calcium hydroxide~~ slightly decreases and the increases due to the formation of hemicarbonates and subsequently monocarbonates. Any further increase in the limestone causes the ~~calcium hydroxide~~CH content to steadily decrease due to dilution of the clinker (~~calcium hydroxide~~CH in these systems is produced due to clinker hydration).

Pore Solution pH

Figure 6 (a) and (b) are plots of the pH of the pore solution of pastes made with PLCs and silica or alumina as predicted by the thermodynamic models. In Figure 6 (a), as the silica content of the pastes is increased, the model predicts that the pore solution pH decreases due to the increased alkali binding and lower initial alkali in pore solution (due to dilution of clinker). Beyond a 20% silica addition by mass, the predicted pH drops rapidly due to the complete consumption of ~~calcium hydroxide~~CH. As the limestone content is increased (up to approximately

2%), the predicted pH slightly increases (due to a reduction in solution volume). When the limestone is greater than approximately 2% the pH decreases due to the initial slight decrease in capillary water (which increases the concentration of hydroxyl ions in solution) and then subsequent dilution of clinker with limestone. In Figure 6 (b), as the alumina content of the pastes is increased, the predicted pH increases due to the reduction in the amount of C-S-H and the formation of stratlingite (stratlingite does not ~~seem to~~ bind Na^+ and K^+ in the model used). As the limestone content in the pastes is increased, the predicted pH slightly increases and then decreases due to the initial slight decrease in the predicted volume of capillary water (which increases the concentration of hydroxyl ions in solution) and then subsequent dilution of clinker with limestone. This behavior is consistent with experimental observations (82).

Influence of Commercial SCMs on Performance Properties of PLC systems

The third part of this work is to study the impact of the addition of commercial SCMs like fly ash, metakaolin, and slag on the performance of ~~OPC~~ cement+~~L~~limestone systems. Simulations are run from limestone fractions of 0% to 30%. The replacement of the ~~OPC~~ ~~L~~cement+limestone binder with commercial SCMs is studied from 0% to 50% replacement by mass.

Fly Ash

Figure 7 contains plots of several performance properties of cementitious pastes made with varying weight fractions of limestone and fly ash (FA). Figure 7 (a) is a plot of the predicted porosity of the hydrated cement paste. As the amount of FA in the system increases, the predicted porosity uniformly increases due to dilution, as seen in experiments (29). When no FA is present,

as the limestone content of the PLC increases from 0% to 2%, the predicted porosity initially decreases from 39% to 34% due to the formation of ettringite and monocarbonate, and if the limestone is increased above approximately 2% the predicted porosity increases due to dilution. When FA is present, the model predicts that the point of minimum porosity increases to higher limestone contents as the alumina in the FA can react with the calcite. This limestone content for minimum porosity is 2% when no FA is present, 3% for a 20% FA content, and 4-5% for a 40% FA content. These predicted trends reflect the near perfect balance of silica and alumina present in fly ash to synergistically react with calcite (limestone) to reduce the porosity.

Figure 7 (b) is a plot of the unreacted calcite present in the paste. The model predicts that ~~As~~ as the amount of FA in the paste increases, the amount of reactive aluminate increases, and hence the amount of reacted calcite increases (and amount of unreacted calcite decreases). The model predicts that the unreacted calcite content follows a bilinear curve, with the unreacted calcite being zero up to the critical limestone content of 2% when no FA is present, 3% at a FA content of 20% and 4-5% for FA contents of 40% and above. Above a FA content of 40%, the maximum amount of limestone that can react as predicted by the model is 5% as the ~~calcium hydroxide~~CH is depleted. Above the critical limestone content, the unreacted calcite is equal to the difference amount of calcite added and the critical limestone content at that FA content. The model predicts that the amount of unreacted calcite increases proportional to the limestone content in the PLC.

Figure 7 (c) is a plot of the predicted ~~calcium hydroxide~~CH content in the paste. The model predicts that ~~As~~ as the amount of FA in the paste increases, the ~~calcium hydroxide~~CH in the paste decreases due to the pozzolanic reactions. The model predicts that for the FA studied, the ~~calcium hydroxide~~CH is completely depleted at a FA content of 40%. An increase in the limestone content

of the PLC slightly decreases the ~~calcium hydroxide~~CH due to the dilution of clinker (approximately 1.5g/100g_{binder} lower CH for a 10% increase in limestone).

Figure 7 (d) is a plot of the predicted pore solution pH in the system. As the amount of FA in the paste increases, the predicted pore solution pH ~~of the pore solution~~ decreases due to an increase in the amounts of alkali binding (more C-S-H is formed with a lower C/S). The model results indicate that ~~An~~ an increase in the limestone content of the PLC slightly decreases the pH due to the dilution of clinker (lower mass of clinker translates to a lower mass of alkalis released into the pore solution).

Metakaolin

Figure 8 contains plots of several performance properties of cementitious pastes made with varying weight fractions of limestone and metakaolin (MK). Figure 8 (a) is a plot of the predicted porosity of the paste. As MK contains a significant fraction of reactive alumina, the model predicts that it is able to react with the limestone and cause a decrease in porosity when CH is present in the system (e.g. the point of minimum porosity, called "critical limestone content", when no MK is present is 2% limestone, and when 15% MK is present is 4% limestone). Below a 15% MK content, if the limestone is increased beyond the critical limestone content, the predicted porosity increases due to dilution. Above a 15% MK content, thermodynamic modeling predicts that the system runs out of CH and stratlingite forms rather than carboaluminate phases (formation of hemi/monocarbonates from alumina requires the presence of ~~calcium hydroxide~~CH (16)), which cause a decrease in porosity as the MK content is increased. The minimum porosity in this region is 24% and occurs at 10% limestone + 40%MK. While this may improve mechanical properties and transport properties by greatly reducing the porosity, there is no CH to buffer against

carbonation and corrosion. When MK>15%, the point of minimum porosity remains at 10% limestone content irrespective of the MK content, and any increase in the limestone content increases porosity due to dilution.

Figure 8 (b) is a plot of the unreacted calcite present in the paste obtained as the output of thermodynamic modeling. As the amount of MK in the paste increases, the model predicts that the amount of reacted calcite first increases and then ~~decreases;~~decreases, which causes the amount of unreacted calcite to first decrease then increase. This appears to be due to reactions of the aluminate from the MK at lower replacement levels (MK<20%) with the carbonates in the limestone to form hemi-/monocarbonates. At higher replacement levels (MK>20%), the model predicts that as the amount of MK increases the amount of ~~C-(A)-S-H~~stratlingite increases in the system and it appears that the aluminate from the MK reacts with the silica present in the metakaolin in the absence of ~~calcium hydroxide~~CH to form ~~C-(A)-S-H~~stratlingite (as it is unable to form hemi-/monocarbonates), which causes the amount of unreacted calcite to increase. The formation of ~~C-(A)-S-H phases like~~ stratlingite in OPC+Ls+MK pastes has been documented in the literature (16). As the amount of limestone in the PLC increases, the model predicts that all calcite that is able to react at a given MK replacement level reacts. Any additional calcite remains unreacted, and the amount of unreacted calcite increases proportional to the limestone content in the PLC.

Figure 8 (c) is a plot of the ~~calcium hydroxide~~CH content in the paste as predicted from thermodynamic modeling. As the amount of MK in the paste increases, the predicted mass of ~~calcium hydroxide~~CH in the paste decreases due to the pozzolanic reactions of the alumina and silica from the MK. The CH is completely depleted when MK>20%. The model shows that ~~An~~ an increase in the limestone content of the PLC slightly decreases the ~~calcium hydroxide~~CH due to the dilution of clinker (approximately 1.5g/100g_{binder} lower CH for a 10% increase in limestone).

Figure 8 (d) is a plot of the pore solution pH in the system, predicted using thermodynamic models. As the amount of MK in the paste increases, the predicted pH of the pore solution decreases due to an increase in the amounts of alkali binding (the model predicts that more C-S-H is formed with a lower C/S) and a decrease in the initial amounts of alkalis in the PLC+MK blend that go into solution. An increase in the limestone content of the PLC slightly decreases the predicted pH due to the dilution of clinker (lower mass of clinker translates to a lower mass of alkalis released into the pore solution).

Slag

Figure 9 contains plots of several predicted performance properties of cementitious pastes made with varying weight fractions of limestone and slag (SL). Figure 9 (a) is a plot of the predicted porosity of the paste. As the amount of SL in the system increases, the predicted porosity remains nearly constant due to the competing effects of (i) dilution, and, (ii) reactions between the CaO, SiO_2, and Al_2O_3 in the SL. When no SL is present, an increase in limestone from 0-2% causes the porosity to drop from 39% to 34%, and an increase in limestone above 2% causes an increase in porosity due to dilution. When SL is present, the model predicts that the alumina in the SL can react with the limestone in the presence of CH to produce carboaluminates and ettringite that decrease the predicted porosity up to a critical limestone content. This critical limestone content as predicted by the model is 2% when no SL is present, 3.5% at a 25% SL content, and 5-6% at a 50% SL content. The minimum predicted porosity is 34-35% and occurs at the critical limestone content. The value of minimum porosity does not appear to be significantly affected by the SL content.

Figure 9 (b) is a plot of the predicted mass of unreacted calcite present in the paste. As the amount of SL in the paste increases, the amount of reactive aluminate increases and hence the model predicts that the amount of reacted calcite increases (and amount of unreacted calcite decreases). Since the addition of even 50% slag does not cause complete consumption of CH according to the model predictions, the reacted limestone increased with increasing slag content (up to 7.5% limestone reacts at a 50% slag content). The model also predicts that ~~As~~ as the amount of limestone in the PLC increases, all calcite that is able to react at a given SL replacement level reacts. Any additional calcite remains unreacted, and the amount of unreacted calcite increases proportional to the limestone content in the PLC.

Figure 9 (c) is a plot of the predicted mass of ~~calcium hydroxide~~CH ~~content~~ present in the paste. As the amount of SL in the paste increases, the predicted mass of ~~calcium hydroxide~~CH in the paste decreases due to the pozzolanic reactions. The model outputs show that ~~This~~ this decrease is much lower than the decrease when FA or MK are used as the slag studied contains a significant portion of calcium that is able to react to form ~~calcium hydroxide~~CH. An increase in the limestone content of the PLC has the following trend: (i) an initial decrease due to the formation of hemi-carbonates instead of C-A-H phases, (ii) a slight increase due to formation of monocarbonates rather than hemicarbonates as more carbonates are available to react in the system (notice that the point of minimum predicted porosity occurs in this same region), and, (iii) a decrease in the ~~calcium hydroxide~~CH due to the dilution of clinker.

Figure 9 (d) is a plot of the predicted pore solution pH in the system. As the amount of SL in the paste increases, the predicted pH of the pore solution slightly decreases due to an increase in the amounts of alkali binding (more C-S-H is formed with a lower C/S). The model predicts that

~~An~~ an increase in the limestone content of the PLC slightly decreases the pH due to the dilution of clinker (lower mass of clinker translates to a lower mass of alkalis released into the pore solution).

CONCLUSIONS

PLC (ASTM C595, Type IL) has been proposed as a direct replacement for OPC (ASTM C150). While ACI 318 and some state highway agencies permit the use of PLC after the 2012 revision of ASTM C595, some agencies have not adopted these cements yet. Questions have been raised on whether the clinker composition (clinkers used to make OPC Type I through V) or SCM use impacts the PLC's performance. This paper uses thermodynamic modeling to address these questions. A variety of limestone and SCM replacement levels in two types of clinker systems have been modeled to obtain properties of the hydrated systems such as porosity, pH, unreacted limestone (as calcite), and CH.

The use of cements with different C_3A contents (lower C_3A cements typical of ASTM Type I/III, and higher C_3A cements typical of Type II/V) ~~clinker~~ to make PLC resulted in nearly identical porosity. For example, the porosity has been calculated as 38%, 34%, and 37% when 0%, 3%, and 15% by mass of limestone is respectively used to replace clinker. The reduction in porosity in PLC systems at low replacement levels ~~has been shown to occur~~appears to be due to the stabilization of ettringite and the formation of hemi/monocarbonate instead of monosulfate.

The performance of 'ideal' SCMs (~~pure~~ 100% alumina and 100% silica) is simulated for limestone contents between 0 and 30%. While thermodynamic models show that both the alumina and silica systems have reduced porosity, the porosity is shown to be lower in the system containing alumina due to the synergistic reactions between alumina and calcite to form

hemi/monocarbonate phases when CH is available, and the formation of stratlingite when CH is depleted. Calcium hydroxide is reduced in both systems due to the pozzolanic reaction, as one may expect, irrespective of the limestone content.

The performance of PLCs is modeled ~~for~~ with three typical commercially available SCMs: fly ash (FA), metakaolin (MK), and slag (SL) for various proportions. The decrease in the predicted porosity is most significant in PLC+MK due to the reactive alumina available. An increase in the amount of SCM in the PLC+FA system causes an increase in the estimated porosity, while an increase in the amount of SL in the PLC+SL system does not have a significant impact on the predicted porosity. The reduction in predicted mass of CH with increasing SCM replacement level is most significant in PLC+MK systems due to the higher pozzolanic reactivity. The model predicts that the decrease in CH is the least in PLC+SL systems due to the large amount of CaO available to react (hydraulically) in the slag. It is also found through modeling that the amount of calcite that reacts when CH is not depleted is roughly proportional to the mass of alumina that is available in the PLC+SCM systems. When CH is depleted, thermodynamic modeling predicts that ~~C-(A)-S-H~~stratlingite phases form as the formation of hemi/monocarbonate phases requires CH as a reactant.

In summary, SCM can be beneficially used with PLC. The model shows that ~~Alumina~~ alumina containing SCMs provide the most synergistic behavior when used with PLC systems. ~~In all scenarios, care must be taken to ensure that~~ CH depletion ~~is not entirely depleted; however, this~~ would only occur at very high replacement levels and not those typically used in ACI 318 or state highway agency applications. As such, thermodynamic modeling shows that PLCs can be used as a replacement for OPCs both without and with SCM. Future works include experimental work to validate the porosity and pore connectivity of pastes containing high volumes of limestone and

SCMs. The current work also only looks at the mean compositions of the typical Type I/III cements (cement A) and Type II/V cements (cement B); future work will include a -Monte-Carlo analysis of studying the variability of the compositions of these clinkers on the variation in the performance parameters of concrete made with PLCs and SCMs.

ACKNOWLEDGMENTS

The authors gratefully acknowledge the financial support provided by ARPA-E (Advanced Research Projects Agency-Energy), CALTRANS (California Department of Transportation), and National Science Foundation (Grant No. NSF CMMI 1728358). The authors gratefully acknowledge support from the John and Jean Loosely Chair and the Edwards Distinguished Chair at Oregon State, which have supported the last two authors respectively. The authors also acknowledge fruitful discussions with Prof. Barbara Lothenbach (EMPA, Switzerland).

REFERENCES

1. Tennis P, Thomas M, Weiss W, "State-of-the-Art Report on Use of Limestone in Cements at Levels of up to 15%," PCA R&D SN3148, Portland Cement Association, Skokie, IL. 2011.

2. Hawkins P, Tennis PD, Detwiler RJ, "The use of limestone in Portland cement: a state-of-the-art review." ENGINEERING BULLETIN 227 ~~ed.~~: Portland Cement Association; 2005.

3. ASTM C150/C150M-19, "~~ASTM C150/C150M-19a~~ Standard Specification for Portland Cement," ASTM International, West Conshohocken, 2019.

4. AASHTO M85, "~~AASHTO M85~~ Standard Specification for Portland Cement," American Association of State Highway and Transportation Officials, Washington DC, 2020.

5. ASTM C595/C595M-20, "~~ASTM C595/C595M-20~~ Standard Specification for Blended Hydraulic Cements," ASTM International, West Conshohocken, 2020~~, pp~~.

6. AASHTO M240M/M240, "~~AASHTO M240M/M240~~ Standard Specification for Blended Hydraulic Cement," American Association of State Highway and Transportation Officials, Washington DC, 2020.

7. Hooton R, Thomas M, "Sulfate Resistance of Mortar and Concrete Produced with Portland-Limestone Cement and Supplementary Cementing Materials: Recommendation for ASTM C595/AASHTO M 240," ~~Book Sulfate Resistance of Mortar and Concrete Produced with Portland-Limestone Cement and Supplementary Cementing Materials: Recommendation for ASTM C595/AASHTO M 240~~, Portland Cement Association, Skokie, IL, USA, Report SN3285a, 2016.

8. Lothenbach B, Kulik DA, Matschei T, Balonis M, Baquerizo L, Dilnesa B, ~~et al.~~Miron GD, Myers RJ, "Cemdata 18: A chemical thermodynamic database for hydrated Portland cements and alkali-activated materials," Cement Concrete Res, V. 115, Jan. 2019, pp. 472-506.

9. Lothenbach B, Le Saout G, Gallucci E, Scrivener K, "Influence of limestone on the hydration of Portland cements," Cement Concrete Res, V. 38, No. 6. 2008, pp. 848-860.

10. Damidot D, Stronach S, Kindness A, Atkins M, Glasser F, "Thermodynamic investigation of the CaO Al2O3 CaCO3 H2O closed system at 25° C and the influence of Na2O," Cement Concrete Res, V. 24, No. 3. 1994, pp. 563-572.

11. Ramezanianpour AM, Hooton RD, "A study on hydration, compressive strength, and porosity of Portland-limestone cement mixes containing SCMs," Cement and Concrete Composites, V. 51. 2014, pp. 1-13.

12. Thomas MD, Hooton RD, "The durability of concrete produced with portland-limestone cement: Canadian studies," PCA R&D SN3142, Portland Cement Association, Skokie, IL. 2010, 28 pp. 28.

13. Matschei T, Glasser FP, "Temperature dependence, 0 to 40 C, of the mineralogy of Portland cement paste in the presence of calcium carbonate," Cement Concrete Res, V. 40, No. 5. 2010, pp. 763-777.

14. De Weerdt K, Kjellsen K, Sellevold E, Justnes H, "Synergy between fly ash and limestone powder in ternary cements," Cement and concrete composites, V. 33, No. 1. 2011, pp. 30-38.

15. Matschei T, Glasser FP, Herfort D, Lothenbach B, "Relationships of Cement Paste Mineralogy to Porosity and Mechanical Properties," International Conference on Modelling of Heterogeneous Materials with Applications in Construction and Biomedical Engineering, 2007.

16. Antoni M, Rossen J, Martirena F, Scrivener K, "Cement substitution by a combination of metakaolin and limestone," Cement Concrete Res, V. 42, No. 12. 2012, pp. 1579-1589.

17. Ashby MF, Cebon D, "Materials selection in mechanical design," MRS Bull, V. 30, No. 12. 2005, 995 pp. 995.

18. Abrams DA, "Design of concrete mixtures, bulletin 1," Structural materials research laboratory Chicago: Lewis Institute. 1918.

19. Bolomey J, "Granulation et prévision de la résistance probable des bétons," Travaux, V. 19, No. 30. 1935, pp. 228-232.

20. Feret R, "On the compactness of the mortars," Annales des Ponts et Chaussées, Série, Vol. 7, Issue No. 4, 1892, pp. 5-164.

21. Lothenbach B, Matschei T, Möschner G, Glasser FP, "Thermodynamic modelling of the effect of temperature on the hydration and porosity of Portland cement," Cement Concrete Res, V. 38, No. 1. 2008, pp. 1-18.

22. Lothenbach B, Winnefeld F, "Thermodynamic modelling of the hydration of Portland cement," Cement Concrete Res, V. 36, No. 2, Feb. 2006, pp. 209-226.

23. Bharadwaj K, Glosser D, Moradllo MK, Isgor OB, Weiss J, "Toward the Prediction of Pore Volumes and Freeze-Thaw Performance of Concrete Using Thermodynamic Modelling," Cement Concrete Res. V. 124, 2019. 124, pp. 105820.

24. Azad VJ, Suraneni P, Isgor O, Weiss W, "Interpreting the pore structure of hydrating cement phases through a synergistic use of the Powers-Brownyard model, hydration kinetics, and thermodynamic calculations," Advances in Civil Engineering Materials, V. 6, No. 1. 2017, pp. 1-16.

25. Glosser D, Azad VJ, Suraneni P, Isgor B, Weiss J, "An extension of the Powers-Brownyard model to pastes containing SCM," ACI Materials Journal, V. 116, No. 5, 2019. 116(5), pp. 205-216.

26. Powers TC, "Structure and physical properties of hardened Portland cement paste," Journal of the American Ceramic Society, V. 41, No. 1. 1958, pp. 1-6.

27. Powers TC, Brownyard TL, "Studies of the physical properties of hardened Portland cement paste," In Journal Proceedings, V~~ol~~. 43, No. 9, 1946, pp. 101-132.

28. Thomas M, "Supplementary cementing materials in concrete." CRC press; 2013.

29. Bharadwaj K, Ghantous RM, Sahan FN, Isgor BO, Weiss J, "Predicting Pore Volume, Compressive Strength, Pore Connectivity, and Formation Factor in Cementitious Pastes Containing Fly Ash," Cement and Concrete Composites, V. 122~~V. In Review.,~~ 2021, pp. 104113.

30. Pichler B, Hellmich C, "Upscaling quasi-brittle strength of cement paste and mortar: A multi-scale engineering mechanics model," Cement Concrete Res, V. 41, No. 5, May. 2011, pp. 467-476.

31. Pichler B, Hellmich C, Eberhardsteiner J, Wasserbauer J, Termkhajornkit P, Barbarulo R, Chanvillard G~~et al.~~, "The Counteracting Effects of Capillary Porosity and of Unhydrated Clinker Grains on the Macroscopic Strength of Hydrating Cement Paste–A Multiscale Model," Mechanics and Physics of Creep, Shrinkage, and Durability of Concrete: A Tribute to Zdeňk P Bažant, 2013, pp. 40-47.

32. Pichler B, Hellmich C, Eberhardsteiner J, Wasserbauer J, Termkhajornkit P, Barbarulo R, Chanvillard G~~et al.~~, "Effect of gel-space ratio and microstructure on strength of hydrating cementitious materials: An engineering micromechanics approach," Cement Concrete Res, V. 45, Mar. 2013, pp. 55-68.

33. Termkhajornkit P, Vu QH, Barbarulo R, Daronnat S, Chanvillard G, "Dependence of compressive strength on phase assemblage in cement pastes: Beyond gel-space ratio - Experimental evidence and micromechanical modeling," Cement Concrete Res, V. 56, Feb. 2014, pp. 1-11.

34. Bentz DP, Ardani A, Barrett T, Jones SZ, Lootens D, Peltz MA, et al., "Multi-scale investigation of the performance of limestone in concrete," Construction and Building Materials, V. 75~~.~~, 2015, pp. 1-10.

35. Bentz DP, Irassar EF, Bucher BE, Weiss WJ, "Limestone fillers conserve cement; Part 1: an analysis based on Powers' model," Concrete international, V. 31, No. 11. 2009, pp. 41-46.

36. de Larrad F, "Concrete mixture proportioning: a scientific approach. Modern Concrete Technology,"~~ Book Concrete mixture proportioning: a scientific approach. Modern Concrete Technology Series~~, ed. A. Bentur und S, Mindess, 1999, 440 pp.

37. Snyder KA, "The relationship between the formation factor and the diffusion coefficient of porous materials saturated with concentrated electrolytes: theoretical and experimental considerations." 2000.

38. Spragg R, Qiao C, Barrett T, Weiss J, "Assessing a concrete's resistance to chloride ion ingress using the formation factor," Corrosion of steel in concrete structures~~, Elsevier~~, 2016, pp. 211-238.

39. Spragg R, Villani C, Weiss J, "Electrical properties of cementitious systems: formation factor determination and the influence of conditioning procedures," Advances in Civil Engineering Materials, V. 5, No. 1. 2016, pp. 124-148.

40. Weiss J, Ley MT, Isgor OB, Van Dam T, "Toward performance specifications for concrete durability: using the formation factor for corrosion and critical saturation for freeze-thaw," Proceedings of the 96th Annual Transportation Research Board, Washington, DC, USA. 2017, pp. 8-12.

41. Weiss WJ, Barrett TJ, Qiao C, Todak H, "Toward a specification for transport properties of concrete based on the formation factor of a sealed specimen," Advances in Civil Engineering Materials, V. 5, No. 1. 2016, pp. 179-194.

42. Weiss WJ, Spragg RP, Isgor OB, Ley MT, Van Dam T, "Toward performance specifications for concrete: linking resistivity, RCPT and diffusion predictions using the formation factor for use in specifications," High tech concrete: Where technology and engineering meet, Springer, 2018, pp. 2057-2065.

43. Archie GE, "The electrical resistivity log as an aid in determining some reservoir characteristics," Transactions of the AIME, V. 146, No. 01, 1942, pp. 54-62.

44. Qiao C, Coyle AT, Isgor OB, Weiss WJ, "Prediction of chloride ingress in saturated concrete using formation factor and chloride binding isotherm," Advances in Civil Engineering Materials, V. 7, No. 1, 2018, pp. 206-220.

45. Garboczi EJ, "Permeability, Diffusivity, and Microstructural Parameters - a Critical-Review," Cement Concrete Res, V. 20, No. 4, Jul. 1990, pp. 591-601.

46. Rajabipour F, "Insitu electrical sensing and material health monitoring in concrete structures," Ph.D. Thesis, Purdue University, West Lafayette, 2006, pp.

47. Moradllo MK, Qiao C, Isgor B, Reese S, Weiss WJ, "Relating formation factor of concrete to water absorption," ACI Materials Journal, V. 115, No. 6, https://doi.org/10.14359/51706844. 2018, pp. 887-898.

48. Qiao C, Moradllo MK, Hall H, Ley MT, Weiss J, "Electrical Resistivity and Formation Factor of Air-Entrained Concrete," ACI Materials Journal, V. 116, No. 3, 2019.

49. Isgor OB, Weiss J, "A nearly self-sufficient framework for modelling reactive-transport processes in concrete," Materials and Structures, V. 52, No. 1, Feb. 2019.

50. Jafari Azad V, Erbektas AR, Qiao C, Isgor OB, Weiss WJ, "Relating the formation factor and chloride binding parameters to the apparent chloride diffusion coefficient of concrete," J Mater Civil Eng, V. 31, No. 2~~.~~, 2019, pp. 04018392.

51. Lothenbach B, Scrivener K, Hooton RD, "Supplementary cementitious materials," Cement Concrete Res, V. 41, No. 12, Dec. 2011, pp. 1244-56.

52. Mehta PK, Monteiro PJ, "Concrete Microstructure, Properties and Materials," McGraw-Hill Education~~Book Concrete Microstructure, Properties and Materials~~, 2006, 684 pp. ~~DOI: 10.1036/0071462899~~

53. Barrett TJ, Sun H, Weiss WJ, "Performance of portland limestone cements: Cements designed to be more sustainable that include up to 15% limestone addition." 2013.

54. Monical J, Unal E, Barrett T, Farnam Y, Weiss WJ, "Reducing joint damage in concrete pavements: Quantifying calcium oxychloride formation," Transportation Research Record, V. 2577, No. 1~~.~~, 2016, pp. 17-24.

55. Suraneni P, Azad VJ, Isgor BO, Weiss WJ, "Calcium oxychloride formation in pastes containing supplementary cementitious materials: Thoughts on the role of cement and supplementary cementitious materials reactivity," RILEM Technical Letters, V. 1~~.~~, 2016, pp. 24-30.

56. Suraneni P, Monical J, Unal E, Farnam Y, Weiss J, "Calcium oxychloride formation potential in cementitious pastes exposed to blends of deicing salt," ACI Materials Journal, V. 114, No. 4., 2017, pp. 631-641.

57. Suraneni P, Salgado N, Carolan H, Li C, Azad V, Isgor B, et al.Ideker J, Weiss WJ, "Mitigation of deicer damage in concrete pavements caused by calcium oxychloride formation–use of ground lightweight aggregates," International RILEM Conference on Materials, Systems and Structures in Civil Engineering, Lyngby, Denmark, 2016, pp. 171-180.

58. Whatley SN, Suraneni P, Azad VJ, Isgor OB, Weiss J, "Mitigation of calcium oxychloride formation in cement pastes using undensified silica fume," J Mater Civil Eng, V. 29, No. 10. 2017, pp. 04017198.

59. Ghods P, Isgor O, McRae G, Miller T, "The effect of concrete pore solution composition on the quality of passive oxide films on black steel reinforcement," Cement and Concrete Composites, V. 31, No. 1., 2009, pp. 2-11.

60. Hou X, Struble LJ, Kirkpatrick RJ, "Formation of ASR gel and the roles of CSH and portlandite," Cement Concrete Res, V. 34, No. 9., 2004, pp. 1683-1696.

61. Hooton R, Thomas M, Ramlochan T, "Use of pore solution analysis in design for concrete durability," Adv Cem Res, V. 22, No. 4., 2010, pp. 203-210.

62. Kulik DA, Wagner T, Dmytrieva SV, Kosakowski G, Hingerl FF, Chudnenko KV, et al., "GEM-Selektor geochemical modeling package: revised algorithm and GEMS3K numerical kernel for coupled simulation codes," Computational Geosciences, V. 17, No. 1., 2013, pp. 1-24.

63. Deschner F, Lothenbach B, Winnefeld F, Neubauer J, "Effect of temperature on the hydration of Portland cement blended with siliceous fly ash," Cement Concrete Res, V. 52, Oct. 2013, pp. 169-181.

64. Dilnesa BZ, Lothenbach B, Renaudin G, Wichser A, Kulik D, "Synthesis and characterization of hydrogarnet Ca3 (AlxFe1− x) 2 (SiO4) y (OH) 4 (3− y)," Cement Concrete Res, V. 59, 2014, pp. 96-111.

65. De Weerdt K, Haha MB, Le Saout G, Kjellsen KO, Justnes H, Lothenbach B, "Hydration mechanisms of ternary Portland cements containing limestone powder and fly ash," Cement Concrete Res, V. 41, No. 3, 2011, pp. 279-291.

66. Matschei T, Lothenbach B, Glasser FP, "Thermodynamic properties of Portland cement hydrates in the system CaO–Al2O3–SiO2–CaSO4–CaCO3–H2O," Cement Concrete Res, V. 37, No. 10, 2007, pp. 1379-1410.

67. Parrot LJ, "Prediction of cement hydration," Proceedings of the British Ceramic Society, 35, 1984, pp. 41-53.

68. Glosser D, Suraneni P, Isgor OB, Weiss WJ, "Estimating reaction kinetics of cementitious pastes containing fly ash," Cement and Concrete Composites, V. 112, 2020, pp. 103655.

69. Glosser DB, "Equilibrium and Non-equilibrium Thermodynamic Modeling of Cement Pastes Containing Supplementary Cementitious Materials," PhD Thesis, Oregon State University, Corvallis, 2020.

70. Taylor HF, "Cement chemistry." Thomas Telford London; 1997.

71. Choudhary A, Ghantous RM, Bharadwaj K, Opdahl O, Isgor OB, Weiss WJ, "Electrical and transport properties of cement mortar made using Portland Limestone Cement," Advances in Civil Engineering Materials, In Review, 2021.~~Choudhary A, Opdahl OH, Ghantous RM, Isgor BO, Weiss JW, "Influence of limestone cement on the electrical and transport properties of cement mortar" ASTM, V. In Review. 2021~~.

72. Zajac M, Rossberg A, Le Saout G, Lothenbach B, "Influence of limestone and anhydrite on the hydration of Portland cements," Cement and Concrete Composites, V. 46~~.~~, 2014, pp. 99-108.

73. Schöler A, Lothenbach B, Winnefeld F, Zajac M, "Hydration of quaternary Portland cement blends containing blast-furnace slag, siliceous fly ash and limestone powder," Cement and Concrete Composites, V. 55~~.~~, 2015, pp. 374-382.

74. Zajac M, Dienemann W, Bolte G, "Comparative experimental and virtual investigations of the influence of calcium and magnesium carbonate on reacting cement," Proceedings of the 13th international congress on the chemistry of cements, Madrid, 2011.

75. Zajac M, Durdzinski P, Stabler C, Skocek J, Nied D, Haha MB, "Influence of calcium and magnesium carbonates on hydration kinetics, hydrate assemblage and microstructural development of metakaolin containing composite cements," Cement Concrete Res, V. 106~~.~~, 2018, pp. 91-102.

76. Schöler A, Lothenbach B, Winnefeld F, Haha MB, Zajac M, Ludwig H-M, "Early hydration of SCM-blended Portland cements: A pore solution and isothermal calorimetry study," Cement Concrete Res, V. 93~~.~~, 2017, pp. 71-82.

77. Bhatty, JI and Tennis, PD, U.S. and Canadian Cement Characteristics: 2004, SN2879, Portland Cement Association, 2008, 67 pp.~~Tennis P, Bhatty J, "Portland cement characteristics-2004," Concrete Technology Today, V. 26, No. 3. 2005, pp. 1-3.~~

78. Azad VJ, Suraneni P, Trejo D, Weiss WJ, Isgor OB, "Thermodynamic investigation of allowable admixed chloride limits in concrete," ACI Materials Journal, V. 115~~.~~, 2018, pp. 727-738.

79. Suraneni P, Hajibabaee A, Ramanathan S, Wang Y, Weiss J, "New insights from reactivity testing of supplementary cementitious materials," Cement and Concrete Composites, V. 103~~.~~, 2019, pp. 331-338.

80. Tennis P, "Chemical and Physical Characteristics of US Hydraulic Cements: 2014," Portland Cement Association, Skokie, Ill. 2016.

81. Poon C-S, Lam L, Kou S, Wong Y-L, Wong R, "Rate of pozzolanic reaction of metakaolin in high-performance cement pastes," Cement Concrete Res, V. 31, No. 9~~.~~, 2001, pp. 1301-1306.

82. Chopperla KST, Smith JA, Ideker J, "The efficacy of portland-limestone cements with supplementary cementitious materials to prevent alkali-silica reaction," Cement, ~~V. Under~~In Review~~.~~, 2021.

TABLES AND FIGURES

List of Tables:

List of Figures:

Figure 6 – pH of the ~~clinker~~ cement+limestone systems with: (a) 100% ~~pure~~ amorphous silica, and, (b) 100% ~~pure~~ amorphous alumina.

Figure 7 – Performance of ~~clinker,~~ cement+limestone and fly ash systems: (a) Porosity, (b) Unreacted Calcite, (c) Calcium Hydroxide Content, and, (d) Pore solution pH.

Figure 8 – Performance of ~~clinker,~~cement+limestone and metakaolin systems: (a) Porosity, (b) Unreacted Calcite, (c) Calcium Hydroxide Content, and, (d) Pore solution pH.

Figure 9 – Performance of ~~clinker,~~cement+limestone and slag systems: (a) Porosity, (b) Unreacted Calcite, (c) Calcium Hydroxide Content, and, (d) Pore solution pH.

Table 1. Compositions of ~~clinkers~~ cements and SCMs used in this study. All values are given in wt. %unless otherwise mentioned.

Constituent	~~Clinker Type I/III~~Cement A (made with clinker used to produce Type I/III cements)	~~Clinker Type II/V~~Cement B (made with clinker used to produce Type II/V cements)	Limestone (Ls)	Fly ash (FA)	Metakaolin (MK)	Slag (SL)
SiO_2	20.00	20.28	0	51.60	49.09	35.23
Al_2O_3	4.79	4.44	0	22.64	40.45	10.79
Fe_2O_3	2.95	3.50	0	8.89	1.45	0.86
CaO	63.31	63.63	0	7.55	0.16	38.65
Na_2O	0.16	0.16	0	1.06	0.09	0.31
K_2O	0.61	0.54	0	2.57	0.16	0.49
MgO	2.16	2.02	0	1.64	0.09	10.75
SO_3	3.52	2.94	0	0.73	0.04	1.52
$CaCO_3$	0	0	100	0	0	0
DOR*	-N/A-	- N/A-	- N/A-	40%	80%	60%
Specific Gravity	3.15	3.15	2.71	2.56	2.36	2.20
C_3S	57.91	59.13	- N/A-	- N/A-	- N/A-	- N/A-
C_2S	13.49	13.18	- N/A-	- N/A-	- N/A-	- N/A-
C_3A	7.68	5.82	- N/A-	- N/A-	- N/A-	- N/A-
C_4AF	8.90	10.63	- N/A-	- N/A-	- N/A-	- N/A-

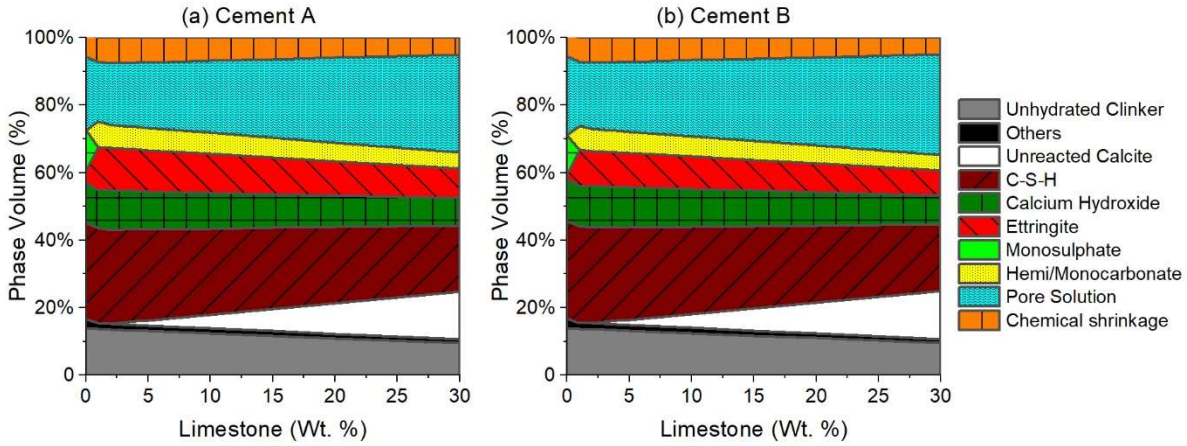

Figure 1. The model predicted **Phase Assemblage of clinker + limestone systems made with (a) ~~typical Type I/III clinker~~cement A (higher C_3A clinker, representative of clinkers used to produce Type I/III cement), and, (b) ~~typical Type II/V clinker~~cement B (lower C_3A clinker, representative of clinkers used to produce Type II/V cement).**

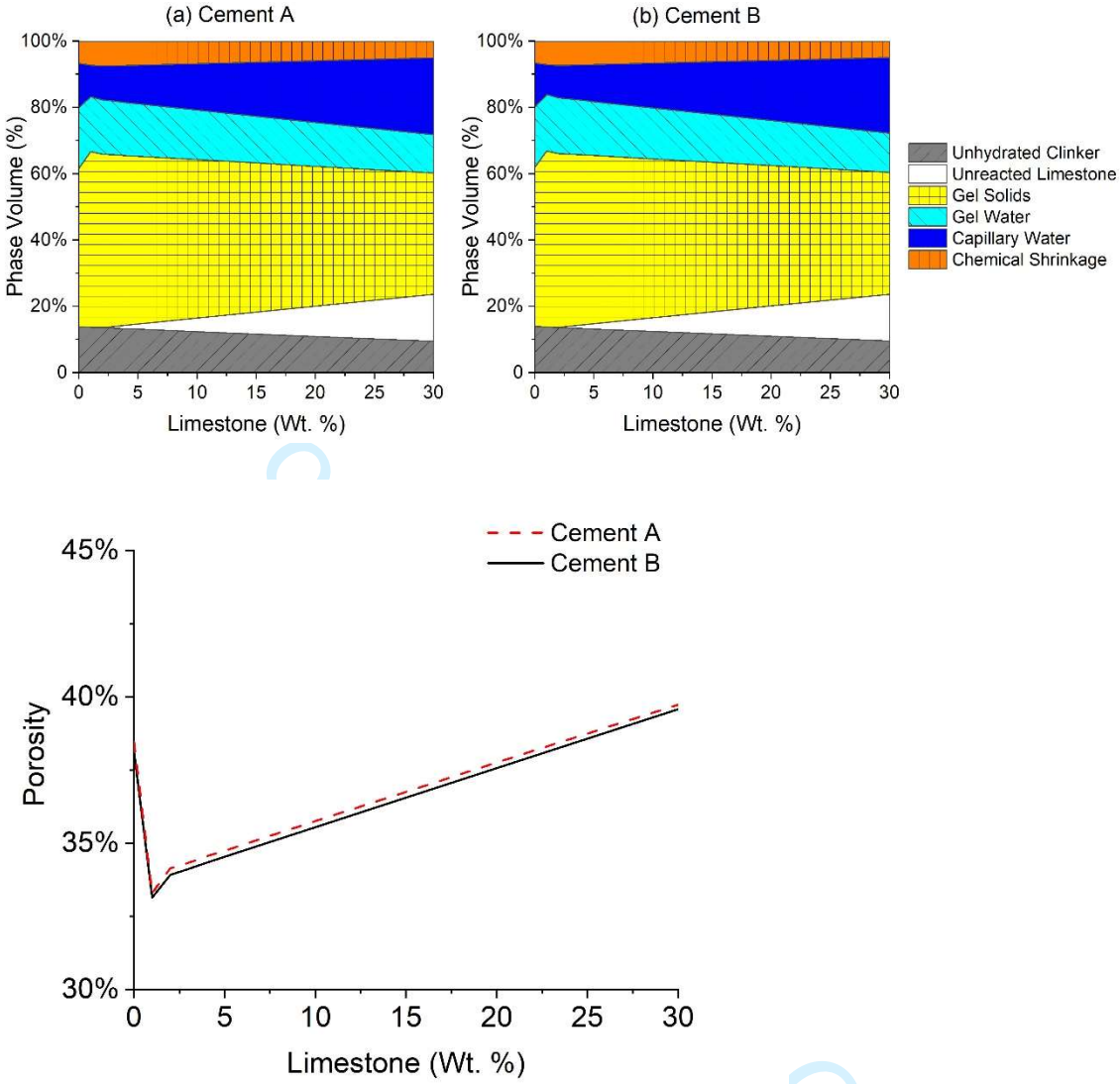

(c) Total Porosity of systems in (a) and (b).

Figure 2. Powers-Brownyard phases of clinker + limestone systems made with (a) ~~typical Type I/III clinker~~cement A (higher C3A clinker, representative of clinkers used to produce Type I/III cement), and, (b) ~~typical Type II/V clinker~~cement B (lower C3A clinker, representative of clinkers used to produce Type II/V cement); (c) Plot of total porosity of the PLC systems made with ~~Type I/III and Type II/V clinker~~cement A and cement B.

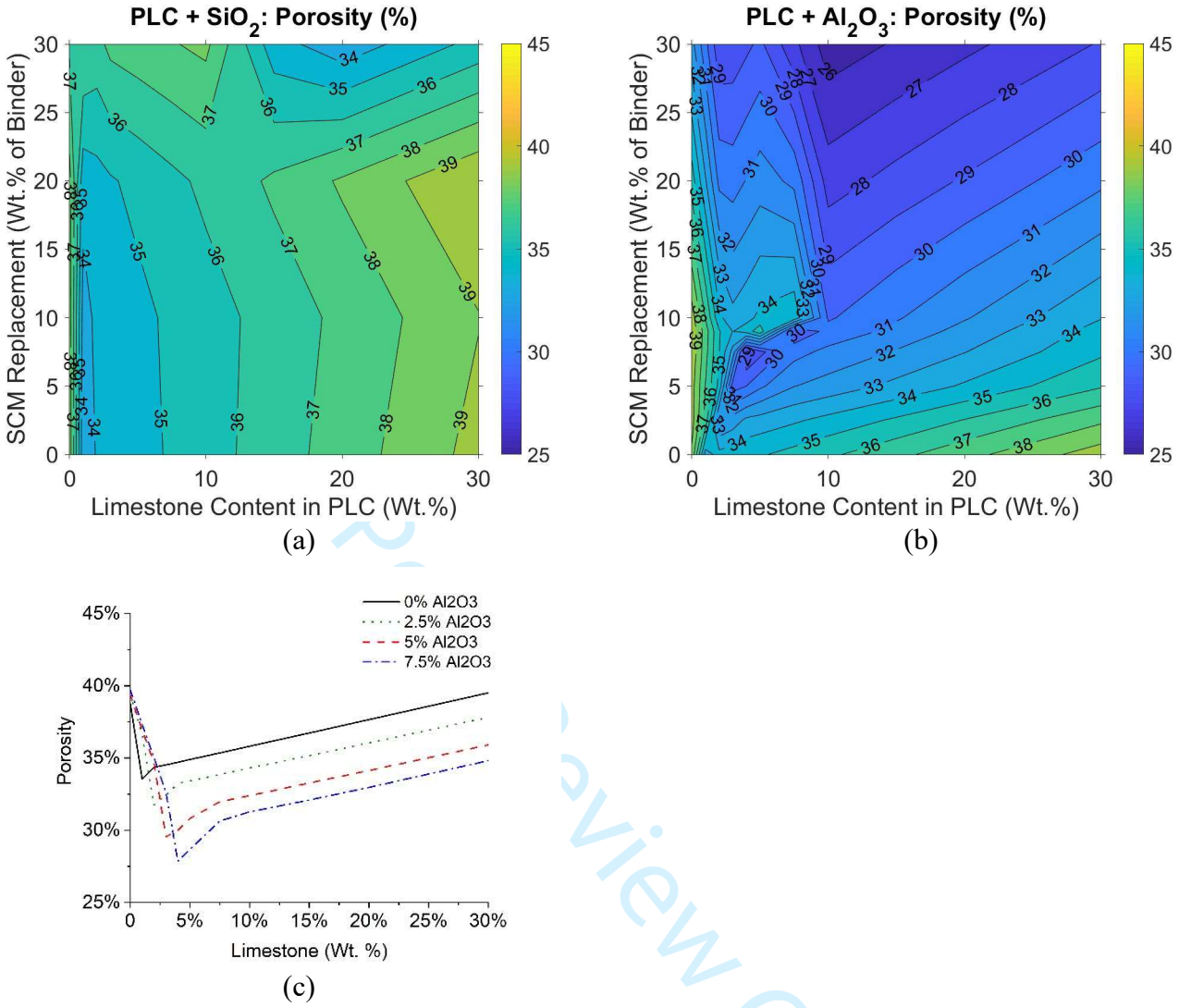

Figure 3. Total porosity of systems made with ~~clinker~~ cement and varying levels of limestone for (a) ~~pure~~ 100% amorphous silica and (b) ~~pure~~ 100% amorphous alumina.

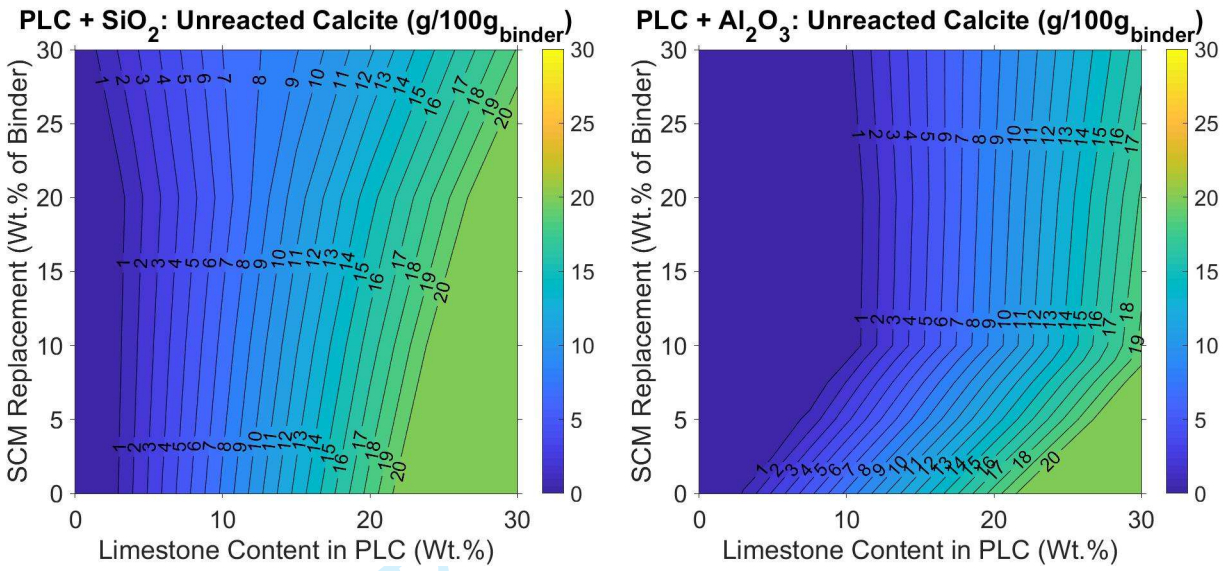

Figure 4. Unreacted calcite in systems made with ~~Type I/II clinker~~cement and varying levels of limestone and (a) 100% ~~pure~~ amorphous silica, and, (b) 100% ~~pure~~ amorphous alumina.

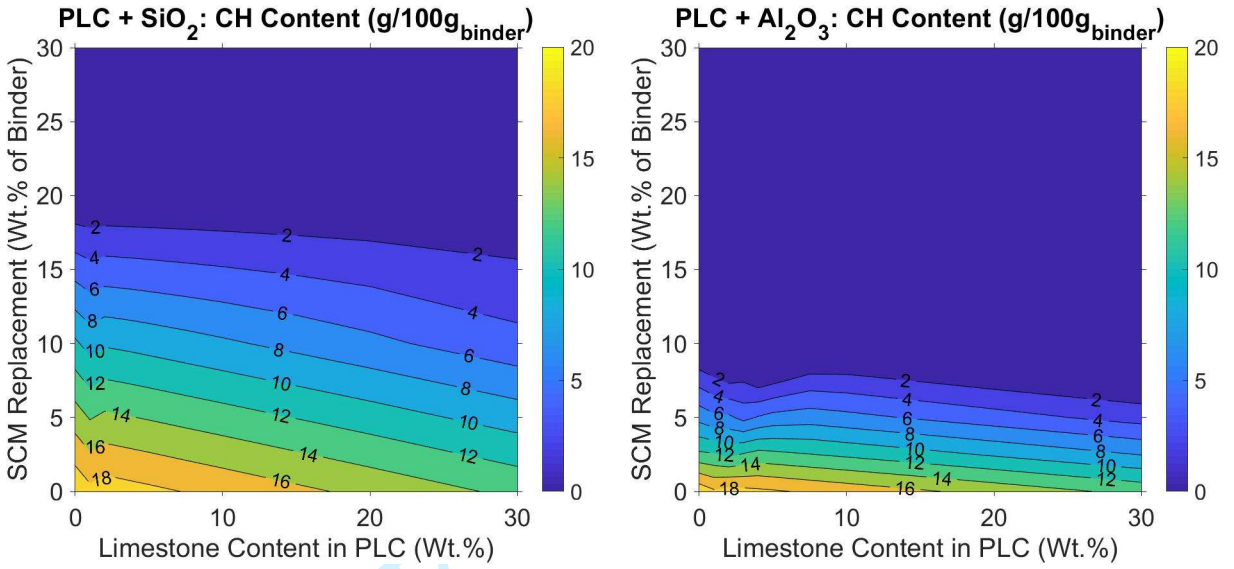

Figure 5. Calcium hydroxide mass in systems made with ~~Type I/III clinker~~cement and varying levels of limestone and (a) 100% ~~pure~~ amorphous silica, and, (b) 100% ~~pure~~ amorphous alumina.

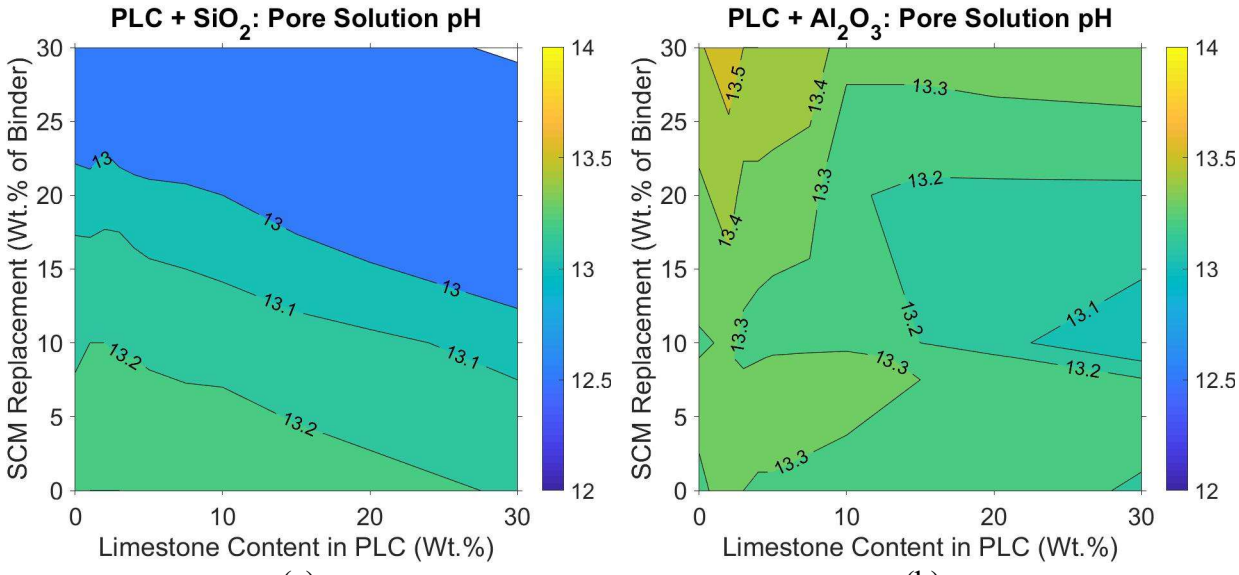

Figure 6. pH of the ~~clinker~~ cement+limestone systems with: (a) 100% ~~pure~~ amorphous silica, and, (b) 100% ~~pure~~ amorphous alumina.

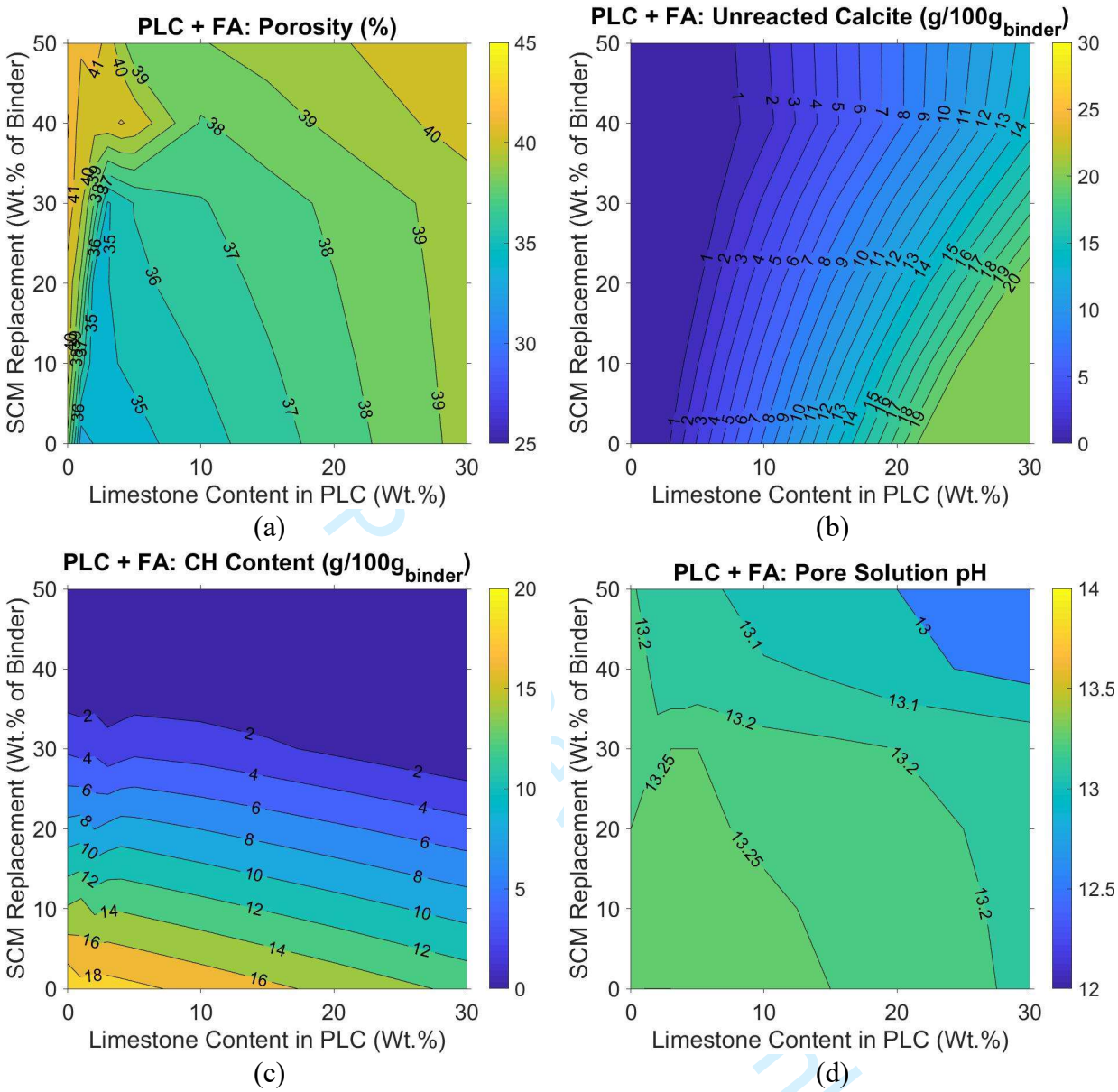

Figure 7. Performance of ~~clinker,~~cement+~~-~~limestone and fly ash systems: (a) Porosity, (b) Unreacted Calcite, (c) Calcium Hydroxide Content, and, (d) Pore solution pH.

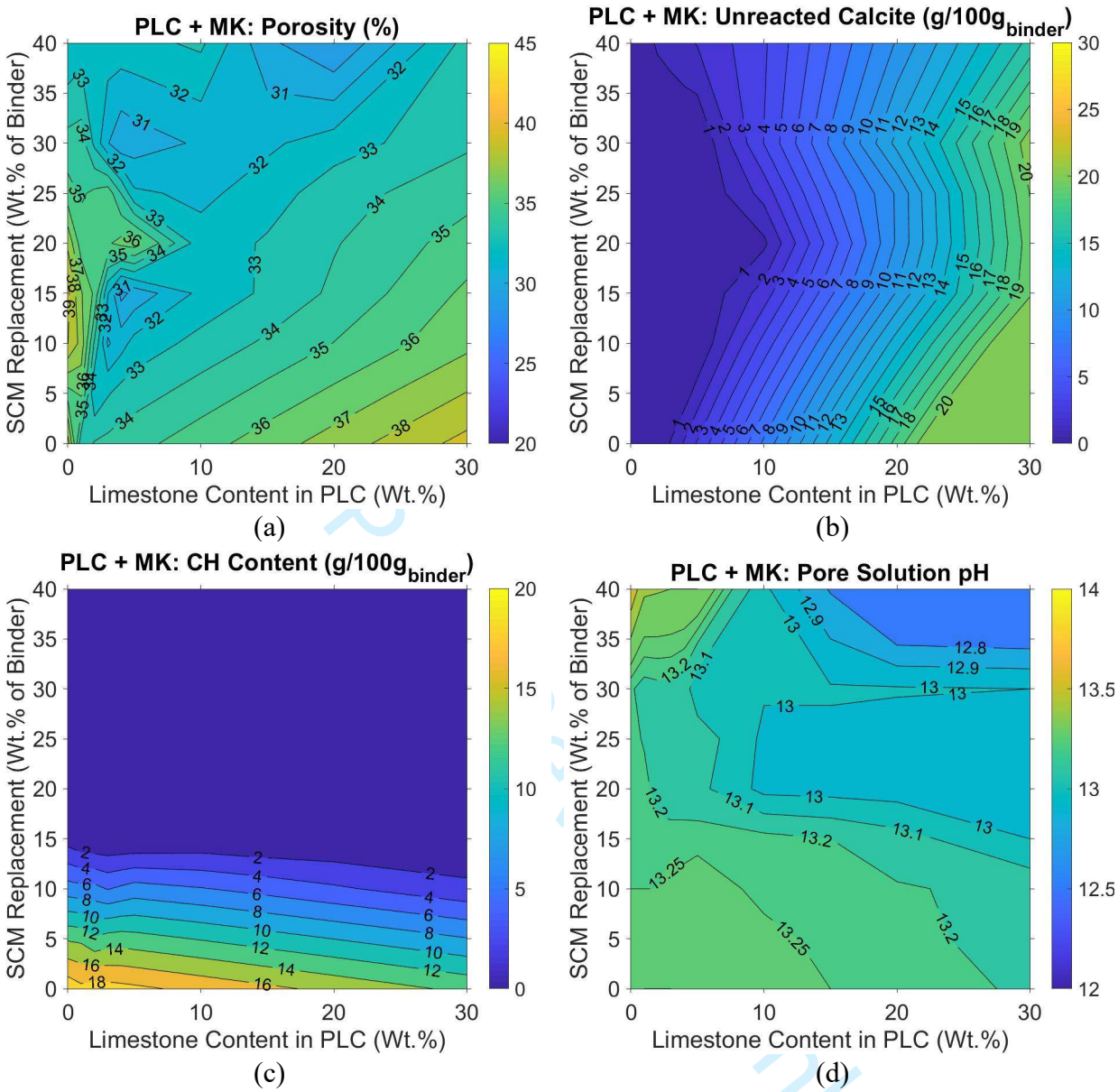

Figure 8. Performance of ~~clinker,~~cement+~~-~~limestone and metakaolin systems: (a) Porosity, (b) Unreacted Calcite, (c) Calcium Hydroxide Content, and, (d) Pore solution pH.

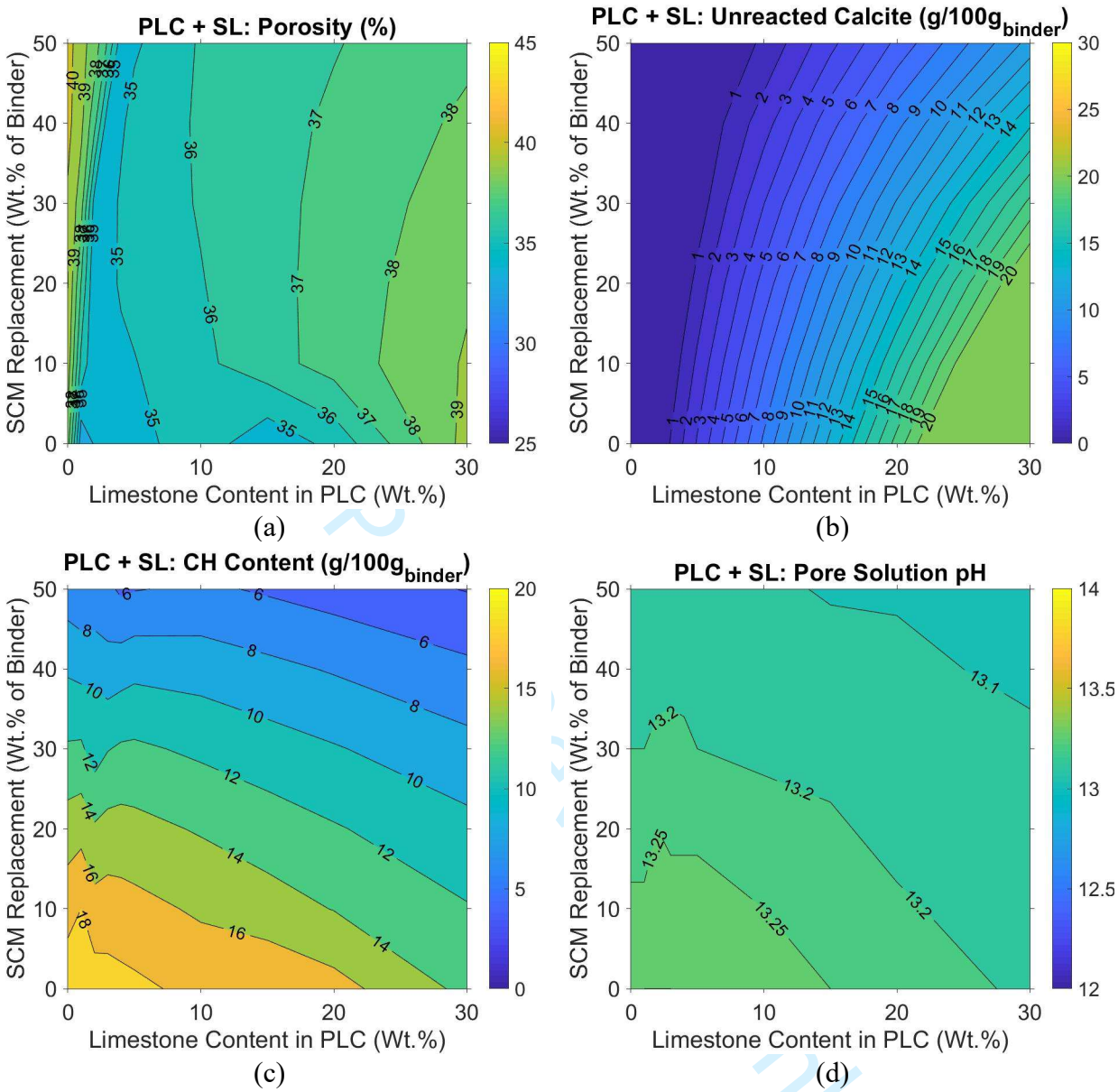

Figure 9. Performance of ~~clinker,~~cement+~~-~~limestone and slag systems: (a) Porosity, (b) Unreacted Calcite, (c) Calcium Hydroxide Content, and, (d) Pore solution pH.

Response to Reviewers

Manuscript Number: M-2021-122

Title: Supplementary Cementitious Materials in Portland Limestone Cements

Authors: Keshav Bharadwaj, O. Burkan Isgor*, W. Jason Weiss;

*Corresponding author, burkan.isgor@oregonstate.edu

Submission Date: 01 April 2021

Review Received date: 03 September 2021

Response to reviews date: 8 October 2021

General Response:

We would like to thank the reviewers for the time they spent to review our manuscript and for their valuable feedback. We hope that questions raised by the reviewers have been addressed in this response document and in the revised manuscript. Our detailed responses to each reviewer's comments are provided below. We are also including a copy of the manuscript with tracking for the reviewers' convenience.

1 Reviewer: 1

(There are no comments.)

Thank you for your time in reviewing the paper.

Response to Reviewers for M-2021-122

2 Reviewer: 2

Comments and Suggestions for the Author(s).

Pg	Ln	Review	Response
		The authors applied thermodynamics model to predict the performance of PLC with different clinker and SCM. This is a necessary step before conducting experimental works to gain fundamental understand. In my opinion, there are some remaining works that can be completed in the future. It is better to add some future works in the conclusion section.	Thank you for these comments. We have updated the conclusions to include future work.

3 Reviewer: 3

Comments and Suggestions for the Author(s) See attached Additional review comments.doc

Pg	Ln	Review	Response
		The IDs "Type I/III clinker" and "Type II/V clinker" are a bit of a misnomer: Type III is a cement defined predominantly by its fineness and sulfate content. This might more accurately classified as the "clinker with the higher alumina content." Further, Table 1 indicates that this would be likely be a Type II cement based on its C3A content, and the	Thank you very much for this comment; we agree that we need to reduce confusion on this. As recommended, we have updated this for clarity. The simulated cements were named to be 'Cement A' for the cement with higher C_3A content and 'Cement B' for the cement with the lower C_3A content as well as included the description of the clinker.

Response to Reviewers for M-2021-122

		"Type II/V clinker" in this paper would NOT meet requirements for Type V cement, but would also be a Type II clinker. Given that some of the results are rather comparable, this is supporting information, but roughty 2% difference in C3A content is not as big of a change as implied by the "Type I/III" vs. "Type II/V" nomenclature here. Suggest these identifiers be changed throughout for accuracy. In addition, the SO3 contents in Table 1 would appear to indicate that these are cement analyses rather than clinker. Recommend the word "clinker" throughout be replaced by "cement" or perhaps "base cement" or something similar. Perhaps simplest would be to replace the IDs with Cement A and Cement B throughout.	For additional clarification, we would like to note that we used the statistics of the compositions of the Type I&III and Type II&V cements from the report "Chemical and Physical Characteristics of US Hydraulic Cements: 2014" by Dr. Paul Tennis to calculate the mean composition of a typical Type I/III and Type II/V cement. This confusion arises as we have combined the statistics of these cements, i.e., lumped all Type I and Type III cements into one class of 'Type I/III cement' and lumped all the Type II and Type V cements into the class of 'Type II/V cement'. However, we understand that the mean values are very similar. A sentence has been added to the conclusions to reflect some of the future work we are working on which includes a Monte-Carlo framework to study the variability of the performance properties due to the variation in the compositions of each type of ASTM cements.
		My other primary concern is that the research results are based on thermodynamic models, good ones and fundamentally sound, but still models, subject to some of the assumptions noted. The results of the	Thank you for pointing this out. We have updated the text to note that the results are model predictions.

Response to Reviewers for M-2021-122

		work should properly be referred to as predictions, estimates, or model outcomes, but tend to be referenced as facts or (implied) results of physical measurements.	
		Since cement pastes and SCMs are being modelled here, the use of "water-to-binder ratio" or w/b throughout is also incorrect. the word "binder" implies fillers are being used, while this research refers to portland-limestone cements and supplementary cementitious materials as the paste ingredients. These are properly referred to using "water-to-cementitious materials ratio" or w/cm.	Thank you for this comment. The authors would like to clarify that the word 'binder' was used as the reactive powder used in the paste and consists of the cement (with limestone contents varying from 0% to 30%) and SCM. This has been more clearly stated in the 'Numerical Investigation' section, and all instances of w/b have been changed to w/cm.
		The word "pure" has connotations that are not useful in this context. Suggest using 100% silica and 100% alumina for accuracy in referring to the model SCMs..	Thank you for this clarification, we have updated the text to call the model SCMs as 100% silica and 100% alumina.
Comments from the attached pdf below			
5	2	Does porosity imply connectivity? My reaction to "porosity and pore volumes" was to consider them similar enough to be redundant.	Thank you for this comment. The 'pore volumes; in this statement was intended to reflect the volumetric distribution of pores, i.e., the volumes of gel pores, capillary pores, air voids etc. As such, the total porosity can be calculated as the sum of the total volumes of these pores. It is worth noting that the pore volumes can be related

Response to Reviewers for M-2021-122

			to the several mechanical and durability properties (e.g., shrinkage, freeze-thaw resistance), the total porosity can be related to other properties (e.g. elastic modulus), and the pore connectivity can be related to the transport properties (e.g. diffusion, sorption, etc). The pore connectivity is not predicted in this work and was as such excluded from this statement. The aim of the statement was to illustrate the gap in the literature and therefore the porosity and pore volumes were listed; the pore connectivity has been added to this sentence as recommended as the influence of limestone on pore connectivity is also a gap in the literature.
5	16	is this a PLC or a OPC-limestone blend? if the latter, the fineness of the limestone is a critical parameter as well.	The systems studied were a cement containing between 0% and 30% limestone by mass, and can be considered a PLC. We have avoided using the word PLC to describe this system as ASTM allows only up to 15% limestone in the PLC while we have studied PLCs with up to 30% limestone.
10	22	Would calcite aragonite and vaterite have different thermodynamic properties here? Was calcite assumed?	This is a very insightful question. The Cemdata 18 thermodynamic database used in this work contains thermodynamic data for the different polymorphs of $CaCO_3$

Response to Reviewers for M-2021-122

			(calcite and aragonite). As such, the GEMS3K algorithm takes into account the polymorphs in the calculation of the stable products that form. In this work calcite was assumed. It should also be noted that while the different polymorphs of $CaCO_3$ (i.e., calcium aragonite, vaterite, and calcite) do have slightly different thermodynamic properties, the predicted reaction products of the simulations are unaffected as the algorithm of GEMS works on the minimization of the system's Gibbs free energy. That is to say, unless any of the polymorphs have a lower specific molar Gibbs free energy than all the reaction products that form in the current simulations (ettringite, carboaluminates & carbonate-ettringite), the reaction products would be unaffected. Additionally, the heat released in the reaction (not shown in this paper) would be affected if different polymorphs are used.
11	9	In the first paragraph here, I think it should be clearly stated that these are predictions from the thermodynamic modelling rather than values determined by direct measurements for example. I have made suggestions	Thank you, we have updated the text.

Response to Reviewers for M-2021-122

		for the first paragraph but the subsequent sections should be carefully reviewed and edited to address this issue.	
12	8	I think this sentence needs further explanation. The gel water remains constant, and the volume of gel-water phases is nearly constant, but the gel porosity is lower? I think I can guess that the relative amount of gel porosity is different for C-S-H and the more crystalline monsulfate and ettringite, but perhaps a sentence to explain that would be helpful just before this one (if that is the right interpretation).	Thank you, we have updated the text to better explain the sentence. You are correct in interpreting the statement. The reduction in the porosity of the hydrated cement gel is due to the formation of lower porosity phases (carboaluminates) at the expense of higher porosity phases (monosulfates). Even though monosulfates are crystalline, they release water upon heating to 105°C, and as such the volumetric water loss is considered to contribute to the volume of gel pores in the system (from Powers-Brownyard's work, Ref. 26, 27 in the paper). Carboaluminates do not typically decompose until 150°C and are not considered to contribute to gel porosity (Ref. 9 in the paper).
12	9	I am familiar with this report and this sentence is slightly misleading: the average limestone content of OPCs that included limestone was 3.1%. Only about 60% (as I recall) of OPCs in the US included limestone. This would make the overall average lower (about 2%). However, I think 3.1% is	Thank you for this clarification. It was our intention to state that the average limestone content of cements containing limestone was 3.1%. The text in the manuscript has been revised.

Response to Reviewers for M-2021-122

		the right value to use here; the statement should just be clarified.	
12	11	based on thermodynamic modelling or based on, say, QXRD measurements from the literature?	This result has been corroborated by both thermodynamic modelling and TGA analysis. For example, Ref. (9) in the paper also shows that there is residual limestone in the hydrated cement pastes made with cement containing 4% limestone by mass.
12	12	This seems to conflict with the previous paragraph. Am I missing something?	Thank you. We acknowledge that there is some conflict here that we missed. The previous paragraph was intended to explain the properties of the system between 0% and 2% limestone contents. This paragraph explains the system properties above a 2% limestone content when the system is diluted due to excess unreacted limestone. The text has been modified to be clearer.
22	21	Since this is modelling work, would it be more accurate to say "appears to be" ?	Thank you. While the predictions of porosity are made with the model, the explanation of the results (porosity reduction due to the formation of ettringite) has been shown experimentally (Ref. 15 in the paper). This said, since these are model predictions without experimental work in this paper, the sentence has been revised.

Response to Reviewers for M-2021-122

34	14	Better reference for this data: Bhatty, JI and Tennis, PD, U.S. and Canadian Cement Characteristics: 2004, SN2879, Portland Cement Association, 2008, 67 pp.	Thank you, the reference has been updated.
		Table 1: Are these analyses based on cements? The SO3 contents might imply that these are cements with added gypsum rather than clinkers.... if so, the terminology of "clinkers" should be corrected to "cement" throughout.	Thank you, the table caption has been revised.
		Figure 1: Here and in the text, it might be assumed that these are experimentally determined volume fractions. I think this needs to be clearly stated as a "predicted" or "estimated" or "calculated" using the modelling approaches described earlier.	Thank you. The text and figure captions have been updated to be more clear.
		Figure 3: Which clinker or cement) was used for Figures 3 through 9? Given that the chemistry was relatively similar, I'm not sure we'd expect much difference, but for completeness, please identify.	Thank you. The cement used was Cement A in the new nomenclature. The caption and text have been updated to be more clear.

Response to Reviewers for M-2021-122

4 Reviewer: 4

Comments and Suggestions for the Author(s)

Pg	Ln	Review	Response
		Interesting work which can be considered for publication after the comments below are addressed.	Thank you for your comments.
3		supplementary cementitious material may be better than supplementary cementing material.	Thank you, the text has been updated.
3		its confusing to say Type I/III and Type II/IV. Could you be more specific?	Thank you. The cement names have been updated to better reflect the compositions. The new nomenclature is 'cement A' and 'cement B', and their compositions are listed in table 1. Cement A is made with the typical clinker that is used to produce Type I and Type III cements in the US. Cement B is made with clinker that is used to produce typical Type II and Type V cements in the US.
3		why should care be taken that calcium hydroxide is not entirely depleted?	Our intention here was to note that the presence of CH provides buffering capacity for the pore solution which consequently aids against the corrosion of steel. The presence of CH also provides some buffer against carbonation damage. We added some qualifiers in the text to make this a bit more clear.

Response to Reviewers for M-2021-122

4		typically when limestone is called an inert material, the consideration is that it isnt pozzolanic or hydraulic - which is true.	Thank you for allowing us to clarify. Hydraulic reactions are chemical reactions that occur between a reactant and water and produce water-stable reaction products. While it is true that limestone does not react pozzolanically, the formation of water-stable carboaluminates is a hydraulic reaction. Therefore, given that a small fraction of the limestone is reacting with aluminates to form carboaluminates, the authors state that limestone is not truly an 'inert' material in the presence of sufficient amounts of alumina.
		Check minor issues with language, spellings, capitalization through the document.	Thank you. We have made several editorial corrections to the document.
6		I understand the modeling with pure silica, but what is pure alumina simulating? Wouldnt simulating calcium aluminosilicate glasses (ideal SCMs) make more sense?	The modelling of pure alumina was done to illustrate the trends of reaction products, porosity etc. that occur when limestone reacts with alumina. Since alumina is one of the components of SCMs, and it is shown that limestone reacts with alumina, the authors felt modelling Al_2O_3 rather than calcium-aluminosilicate glasses (which are combinations of SiO_2+CaO+Al_2O_3) would provide a more fundamental understanding of the reactions that take place in the PLC-SCM system to

Response to Reviewers for M-2021-122

			the reader. Additionally, using aluminous SCMs are common in the state of California in the US and the alumina simulations apply strongly to metakaolin.
		There is a lot of work from Karen Scrivener's group that you may consider citing. Considering the cost of metakaolin, running similar simulations with calcined clays (40 to 70% kaolinite content), might be a fruitful exercise.	Thank you for this suggestion. The authors would like to note that we have cited several papers from Prof. Scrivener's group (Ref. 9, 16, 51 in this paper). While the cost of metakaolin is certainly an important parameter, the scope of this paper was to illustrate that PLCs can be used as direct replacements to OPCs with and without SCMs. For this study, the SCMs studied represented the wide range of chemistries of typical commercial SCMs.
8		I am a little confusing with the MPK model. If you consider Type I vs. Type III cements, a major difference is the fineness. How is this considered in the MPK model? In addition, its not only S, A, and C that react. You can and will have Mg phases react in slag for example. It may be good to acknowledge some limitations of the model in P8.	Since the scope of this paper was to study the impact of replacement o OPC with PLC, only a brief overview of the MPK model was noted in this paper. The MPK kinetic model (Ref 68,69 in this paper) includes fineness of the cement and SCM as an input to the model. The input to the thermodynamic model also includes all the minor oxides which includes MgO. For example, the model predicts in these simulations that the MgO phases react to

Response to Reviewers for M-2021-122

			form brucite and if a large amount of MgO is present, hydrotalcite. Text has been added to include some limitations of the MPK kinetic model such as particle packing etc.
9		Calling MgO and SO3 alkali oxides is confusing.	Thank you. The text has been updated to 'minor oxides'.
9		so the limestone fineness doesnt affect reaction kinetics? so what explains the massive differences that limestone fineness has at all ages in published literature?	Thank you for the opportunity to clarify this. We actually do not make this claim in this paper. In fact, it is true that the fineness of limestone has an impact on the performance properties of cementitious system. Note that typically in the US, PLCs are ground to a fineness such that the performance of concrete made with PLCs at 28-days is equivalent to the performance of concrete made with OPCs. However, studying the effect of the fineness of the cement is beyond the scope of this paper. The kinetic model used (MPK model) accounts for the fineness of the powders used in the mixture. However, the simulations were all run at the same fineness as the variable that objective of this paper was to study the impact of limestone content of PLCs on their performance. While the model does allow for varying the fineness, the combined effects of reaction of limestone and

Response to Reviewers for M-2021-122

			kinetics of hydration make the results of the model harder to explain.
11		please comment on fineness effects here (cement, limestone, SCM).	Thank you. Text has been added to comment on the fineness.
11		Why 56-days? Class F fly ash (which is what you are testing) would not have reacted much at 56 days.	Thank you. 56-days was chosen as it allows for pozzolanic reaction to study the impact of limestone on the cement+SCM systems, and as this is the usual age for testing concrete containing SCMs to allow for sufficient SCM reaction. While it is true that Class-F fly ashes continue to react beyond 56-days, and in some cases this reaction can be significant, there is also experimental evidence (see references 14 and 63) which indicate that significant reaction of Class-F fly ashes can occur around 56 days, and mostly before 90 days.
		Table 1: The DOR* is the reactivity of the SCM in a reactivity test, right? Of I understand right (P8, 9), this is the SCM amorphous content. If so, the DOR* values in Table 1 make no sense to me. FA is typically 60 to 80% amorphous, and MK and SL are typically 95%+ amorphous. Please explain the details of your calculation because this is confusing.	Thank you for allowing us to clarify this. The DOR* is the maximum degree of reactivity of an SCM, which is the maximum mass fraction of the SCM that can react at equilibrium with excess CH and water present. A statistical analysis of the DOR* of FAs in the literature tested for reactivity indicates that the average reactivity of typical FAs used in the US is 40% and that of typical slags used in the

Response to Reviewers for M-2021-122

			US is 60%. It is also worth noting (from Ref. 69) that the average amorphous content of FAs in the US is 50%-60%, obtained from XRD (Ref. 69). While the amorphous content is related to the DOR*, the DOR* depends on other parameters such as how the reaction products occlude the phases and the particle size and shape.
		Figure 1, how do you account for limestone filler effect?	Thank you. The MPK model considers the fineness of the components of the cementitious mixture, and therefore, does partly account for the filler effect. However, it should be noted that the filler affect is predominantly seen at early ages, at the ages studied in this paper, we don't expect it to be a significant factor (though a slight variation may exist) at later ages studied. This is shown in the reference item below. **Reference:** Igor De la Varga (2013) "Increased fly ash volume and internal curing in concrete structures and pavements", Ph.D. Thesis, Purdue University, West Lafayette, USA.
		You may want to point out that ref. 80 is 7 years old, and this number is likely not true now.	Thank you for this note. The authors would like to note that this is a report that is part of a series of reports that is published every 10 years, and as such, contains the most up-to-date data for cement

Response to Reviewers for M-2021-122

			chemistries. Personal communication with the author(s) of the upcoming report indicate that a limestone content of around 3% is still relevant to this day.
13		yes above 3-4% limestone, it will not react. But it will increase the cement hydration due to filler effect, which will increase gel solids and gel water.	Thank you. The filler effect is partly accounted for to some extent in the MPK model. However, it should be noted that the filler affect is predominantly seen at early ages. This is shown in the reference item below. **Reference:** Igor De la Varga (2013) "Increased fly ash volume and internal curing in concrete structures and pavements", Ph.D. Thesis, Purdue University, West Lafayette, USA
17		is the alumina reaction consuming twice the CH of the silica reaction in line with stoichiometry?	Thank you. Yes, this reaction is stoichiometric as the reaction of alumina to form carboaluminates consumes twice the CH as the reaction of SiO_2 to form C-S-H.
		Perhaps I am not understanding, but what is the degree of reaction of the SCM used in Figure 7? Is this the same as DOR*? How do you account for the relationship between reactivity and replacement (inverse relationship)?	The degree of reaction is the mass fraction of the SCM that has reacted in the system (56-days). The DOR* is the maximum degree of reaction that the SCM can show at equilibrium (infinite time).

			For the replacement levels and reactivities studied, the authors believe that this inverse relationship between the reactivity and replacement level that the reviewer notes does not affect the calculations to a significant degree.
		How is binder defined in Figure 7 (clinker + SCM + limestone)?	Thank you. The word 'binder' has been clarified in the manuscript per recommendations from Reviewer 3. The word 'binder' was intended to mean the reactive powder containing cement+limestone, and the phrase 'cementitious powder' is used to mean 'cement+limestone+SCM'.
		I am really quite confused by Figure 7 results. It is stated that calcium hydroxide is depleted at 40% fly ash replacement level. But this is not remotely true and contradicts literature. Your own work, for example, ref. 55 shows considerable amounts of calcium hydroxide even at 60% fly ash replacement levels. Other papers from Scrivener, yet other papers dealing with HVFA all show that a good amount of calcium hydroxide remains in the system at 60% fly ash replacement. What you are showing, at 0% limestone, is that	Thank you for this comment. CH consumption depends on several factors such as the chemistry of the FA, the reactivity of the fly ash, and the degree of reaction (age) of the system studied. CH consumption in experiments also depends on the local availability of CH for pozzolanic reaction. Thermodynamic models cannot account for CH that is not available to react; therefore, it is possible to have some disparity between experimental and modelling results. This has been noted in the paper as a limitation of the model that the model assumes all the CH is available to react at the given time,

Response to Reviewers for M-2021-122

		calcium hydroxide contents are halved at 20% fly ash replacement. I dont think this is accurate or in line with experimental data. Please check what is happening. If these are the results, please point out that it contradicts a wealth of experimental data.	and some CH may remain in the system due to local availability effects (see Ref. 55). It is also likely that Reference 55 likely used a low reactivity fly ash and had a low w/cm which limited the degree of reaction of the system. Additionally, the FAs used in Ref 55 contained a significant amount of CaO (>13% in most cases) while the FA in this study contains only 7.5% CaO. It should also be noted that there are also references that indicate CH depletion. For example, Reference 29 shows that at 56 days, a significant portion of the CH is depleted in a 20% FA system.
		I dont know that Figure 8 is accurate either, and a comparison with literature is needed. MK is super fine, and beyond a certain replacement level, its degree of reaction drastically reduces. I dont think you will get 0 CH at 18% MK replacement level.	Thank you. The results shown are model predictions and the model predictions correlate well with other model predictions from the literature (see Ref. 51, 75). As noted in the previous, we also acknowledge that thermodynamic models cannot account for CH that is not available to react; therefore, it is possible to have some disparity between experimental and modelling results.

Response to Reviewers for M-2021-122

			However, we also note that there are experimental observations in the literature which also show near complete depletion of CH in OPC+MK pastes (see Ref. 16 and Proceedings of the 1st international conference on Calcined Clays for Sustainable Concrete).
		Figure 9: Odd results for CH again. Slag consumes plenty of CH in cement pastes. Most authors have not shown a huge difference between CH contents in fly ash and slag pastes (see again ref. 55 for example). So why do you see massive differences?	Thank you; while it is true that some slags may consume plenty of CH, the CH consumed depends on the chemistry of the slag, the reactivity of the slag, and the degree of reaction of the slag at that age among other parameters. There is evidence in the literature (see ref. 51) that slags typically consume less CH than class-F FAs. The reference also shows that slag systems have CH contents only moderately lower than OPC systems. The simulations in this paper reflect the slag composition used in the study.
		Considering this is modeling only, experimental validation is missing. Which could be ok, but a very careful comparison of your results with literature is needed. Right now this is missing. In addition, do consider adding language about assumptions and limitations.	Thank you. The text has been updated carefully to reflect that these results are the predictions of the model. Future works have also been added to the conclusions.